Study on Redox Reaction of Viologens as Probes of Micro-environments in Nafion Films on Au electrode

金電極上のナフィオン膜中におけるミクロ環境プローブとしてのビオロゲンの酸化還元反応に関する研究

October 2020

2020 年 10 月

Department of Advanced Technology and Science for Sustainable Development,
Graduate School of Engineering, Nagasaki University

長崎大学大学院工学研究科グリーンシステム創成科学専攻

Tatsuya Ayabe

綾部　達也

Contents

Abstract

Proton transporting membranes have been among the fundamental materials supporting a variety of modern electrochemical devices and sensors. The most frequently used one is Nafion®. The Nafion films have found many applications for proton transportation, energy storage, energy conversion, and catalytic reaction media.

A Nafion film immersed in water has a phase-separated structure composed of a micro water-phase and a perfluoroalkyl-phase. The water phase is in a hydrophilic ionic channel as a microscopic water-domain surrounded by walls with condensed sulfonate groups of the side chains. The perfluoroalkyl-phase is a bulk region composed of perfluoroaklyl chains of Nafion. Because of the characteristic water-phase micro-network structures, chemical micro-environment in a Nafion film has a specific electrostatic and hydrated nature. Studies on the basis of the two-phase framework model with the water-phase and perfluoroalkyl-phase were extensively conducted through various approaches from a viewpoint of micro-structures of hydrated Nafion films. Using the results of spectroscopic measurements of hydrated Nafion films by X-ray reflection and scattering and neutron-ray diffraction, a variety of nanoscopic and mesoscopic structure models have been proposed.

The spectroscopic methods frequently have difficulty in gaining a better insight into the micro-phase structures in the hydrated Nafion films. On the other hand, analytical methods using redox probes can attain in-situ observation of chemical micro-environments in the hydrated Nafion films. Viologens as redox probes uncovered the ionic channel sizes in Nafion films from the diffusion and dimerization processes of the probes. Viologens exhibited superior molecular probe features, because they have reversible electrochemical activity. Both oxidized (V^{2+}) and one-electron reduced ($V^{\bullet+}$) forms are cationic species possessing affinity to the anionic sulfonate groups in the ionic channel of Nafion. Strongly colored nature of $V^{\bullet+}$ forms enables us to follow the state of viologen by visible spectroscopies. To our best knowledge, however, redox probes have been restricted so far to cationic and hydrophilic ones, which are perfluoro-repulsive. This has limited the obtainable properties of the micro-environments in Nafion. To shed light in more depth of the ionic channels, the use of a probe having a perfluoroalkyl affinity should be meaningful. In this part, I have analyzed phase separation structures of a perfluoro sulfonic polymer, Nafion®, using a newly

synthesized redox probe bearing short fluoroalkyl chain, N,N'-di-(1H,1H,2H,2H-perfluorobutyl)-4,4'-bipyridinium dichloride (FC4VFC4) with an intension to introduce interaction with fluoroalkyl region of Nafion® film. First, the effect of fluorination on the aqueous solution electrochemistry was a investigated using voltammetric measurements and DFT computations. The formal potential of one-electron transfers redox couple, viologen radical monocation/dication, became 128 mV less negative upon fluorination, and the diffusion coefficient of the oxidized form was lowered by ca. 12%. Calculations indicated that the shift of the formal potential is largely caused by strong electron-withdrawing nature of the perfluorinated groups despite a separation of $(CH_2)_2$ from the viologen core. The effect is counter balanced by an opposite but smaller effect from the change of solvation free energy due to perfluorination.

For exploring the Nafion® film micro-phase separation structure, the electrochemistry of FC4VFC4 in a Nafion® film on an Au electrode has been explored. The capability of FC4VFC4 were highlighted as a redox-active probe for chemical micro-environments of the separated phases in the Nafion® film by clarifying the difference of its electrochemical behavior from that of its alkyl analog, dibutyl viologen (C4VC4). The strongly concentration-dependent time change revealed the formation of an aggregate of FC4VFC4 in the ionic channels in the Nafion® film. The aggregate blocks its own redox reaction at higher solution concentrations than 10 μM, although at 5 μM, FC4VFC4 exhibited a quasi-reversible response. In contrast, C4VC4 showed a quasi-reversible response in the concentration range from 5 μM to 500 μM. I also used the time dependent change of electroreflectance (ER) spectra to track the state of viologens in the close proximity of the electrode|Nafion interface.

To sum up, I proposed an unprecedented model that describes the behavior of FC4VFC4 in the ionic channel in the Nafion® film. The aim of this study is at the exploration of the microenvironment of Nafion using viologens, including a newly synthesized perfluorinated viologen, as redox probes. I used the results of electrochemical and electroreflectance (ER) spectral measurements to describe the behavior of the viologens in the Nafion film and at the electrode/organic monolayer/Nafion interface.

This thesis consists of seven chapters. Introduction to this doctoral dissertation research is given in Chapter 1. Chapter 2 is a review of the nature of fluoroalkylation and perfluorinated sulfonic-acid ionomer. Chapter 3 details experimental methods.

In Chapter 4, I have analyzed phase separation structures in the Nafion film using the new redox probe bearing short fluoroalkyl chain, N,N'-di-(1H,1H,2H,2H-perfluorobutyl) -4,4'-bipyridinium dichloride (FC4VFC4) with an intension to introduce interaction with fluoroalkyl region of Nafion film. First, the effect of fluorination of viologen on the aqueous solution electrochemistry was investigated using voltammetric measurements and DFT computations. The formal potential of one-electron transfers redox couple, viologen radical monocation/dication, became 128 mV less negative upon fluorination, and the diffusion coefficient of the oxidized form was lowered by ca. 12%. Calculations indicated that the shift of the formal potential is largely caused by strong electron-withdrawing nature of the perfluorinated groups despite a separation of $(CH_2)_2$ from the viologen core. The effect is counter balanced by an opposite but smaller effect from the change of solvation free energy due to perfluorination.

In Chapter 5, the electrochemistry of FC4VFC4 in a Nafion film on an Au electrode has been investigated. The capability of FC4VFC4 were highlighted as a redox-active probe for chemical micro-environments of the separated phases in the Nafion film by clarifying the difference of its electrochemical behavior from that of its alkyl analog, dibutyl viologen (C4VC4). The strongly concentration-dependent time change revealed the formation of an aggregate of FC4VFC4 in the ionic channels in the Nafion® film. The aggregate blocks its own redox reaction at higher solution concentrations than 10 μM, although FC4VFC4 exhibited a quasi-reversible response at 5 μM. In contrast, C4VC4 showed a quasi-reversible response in the range from 5 μM to 500 μM. The time dependent change of ER spectra was used to take a close look at the proximity of the electrode|Nafion interface.

In Chapter 6, I focused on the interfacial structure between Nafion and self-assembled monolayer (SAM) on a Au electrode. I used SAMs possessing various terminal groups and unveiled the relationship between SAM surface properties and Nafion structure on the basis of the observation of the electrochemical behavior of methyl viologen.

In Chapter 7, I summarized the thesis and described the perspectives on the chemical micro-environments of Nafion films obtained in this thesis study.

Acknowledgments

While there are a number of individuals to whom I would like to express my utmost gratitude and appreciation, below I would like to single out those who made the most valuable contribution.

Throughout the course of this study, the patience, encouragement and mentorship provided by Professor T. Sagara is greatly deserving of recognition. Prof. Sagara has taught me many things including science and beyond to which I will be always grateful. Simply, many thanks for everything.

For immense help and extremely fruitful discussions during my studies and research, I would like to express sincere thanks to Associate Professor H. Murakami

Sincere thanks also go to Assistant Professor H. Tahara for many helpful advice valuable discussions in this project.

I wish to thank Assistant Professor B. Chan for his valuable discussions and technical assistance in DFT calculations.

Special thanks to Mrs. N. Yuki for many help and support, simplifying my efforts.

The excellent working environment established by the people of the Sagara lab group, I would like to thank them each for their friendship throughout my time in Nagasaki.

For fulfilling experience of oversea research program and worthful corporation to collective writing, I would like to show my greatest appreciation to Prof. A. Chan and the Chan lab group members.

Finally, thank you to my parent for their support of my life.

Chapter 1

Introduction

1.1. Background

An ion exchange membrane (IEM) is one of the most broadly used functional materials for various applications [1]. The selectivity of IEM that allowed permeation of a specific ion is indispensable for some traditional processes such as electrodialysis, and it has high advantages for energy conversion and production such as fuel cells and redox flow batteries [2].

Proton transporting membranes have been among the fundamental materials supporting a variety of modern electrochemical devices and sensors. The most frequently used one is Nafion [3] (Fig. 1-1.). Nafion films have found many applications for proton transportation, energy storage, energy conversion, and catalytic reaction media.

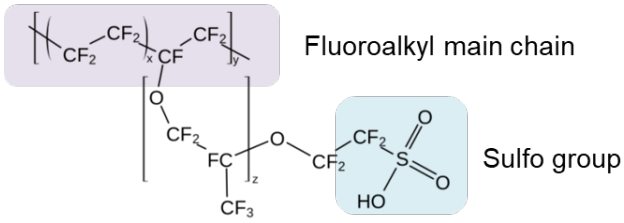

Fig. 1-1. Nafion Chemical strucutre

A Nafion film immersed in water has a phase-separated structure composed of a micro water-phase and a perfluoroalkyl-phase. The water phase is in a hydrophilic ionic channel as a microscopic water-domain surrounded by walls with condensed sulfonate groups of the side chains. The perfluoroalkyl-phase is a bulk region composed of perfluoroaklyl chains of Nafion. Because of the characteristic water-phase micro-network structures, chemical micro-environment in a Nafion film has a specific electrostatic and hydrated nature. Studies on the basis of the two-phase framework model with the water-phase and perfluoroalkyl-phase were extensively conducted through various approaches from a viewpoint of micro-structures of hydrated Nafion films. Using the results of spectroscopic measurements of hydrated Nafion films by X-ray reflection and scattering and neutron-ray diffraction, a variety of nanoscopic and mesoscopic structure models have been proposed.

The spectroscopic methods frequently have difficulty in gaining a better insight into the micro-phase structures in the hydrated Nafion films. On the other hand, analytical methods using redox probes can attain in-situ observation of chemical micro-environments in the hydrated Nafion films. Viologens as redox probes uncovered the ionic channel sizes in Nafion films from the diffusion and dimerization processes of the probes. Viologens exhibited superior molecular probe features, because they have reversible electrochemical activity. Both oxidized (V^{2+}) and one-electron reduced ($V^{\bullet+}$) forms are cationic species possessing affinity to the anionic sulfonate groups in the ionic channel of Nafion. Strongly colored nature of $V^{\bullet+}$-forms enables us to follow the state of viologen by visible spectroscopies. To our best knowledge, however, redox probes have been restricted so far to cationic and hydrophilic ones, which are perfluoro-repulsive. This has limited the obtainable properties of the micro-environments in Nafion. To shed light in more depth of the ionic channels, the use of a probe having a perfluoroalkyl affinity should be meaningful.

1.2. Objective

The aim of this study is at the exploration of the microenvironment of Nafion using viologens, including a newly synthesized perfluorinated viologen, as redox probes. I used the results of electrochemical and electroreflectance (ER) spectral measurements to describe the behavior of the viologens in the Nafion film and at the electrode/organic monolayer/Nafion interface.

1.3. Scope of the Thesis

This thesis consists of seven chapters. Introduction to this doctoral dissertation research is given in this Chapter. Chapter 2 is a review of the nature of fluoroalkylation and perfluorinated sulfonic-acid ionomer. Chapter 3 details experimental methods.

In Chapter 4, I have analyzed phase separation structures in the Nafion film using the new redox probe bearing short fluoroalkyl chain, *N*,*N*'-di-(1*H*,1*H*,2*H*,2*H*-perfluorobutyl) -4,4'-bipyridinium dichloride (FC4VFC4) with an intension to introduce interaction with fluoroalkyl region of Nafion film. First, the effect of fluorination of viologen on the aqueous solution electrochemistry was investigated using voltammetric measurements and DFT computations.

In Chapter 5, the electrochemistry of FC4VFC4 in a Nafion film on an Au electrode has been investigated. The capability of FC4VFC4 were highlighted as a redox-active probe for chemical micro-environments of the separated phases in the Nafion film by clarifying the difference of its electrochemical behavior from that of its alkyl analog, dibutyl viologen (C4VC4). The time dependent change of ER spectra was used to take a close look at the proximity of the electrode|Nafion interface.

In Chapter 6, the interfacial structure between Nafion and self-assembled monolayer (SAM) on a Au electrode was focused. I used SAMs possessing various terminal groups and unveiled the relationship between SAM surface properties and Nafion structure on the basis of the observation of the electrochemical behavior of methyl viologen.

In Chapter 7, this thesis is summarized with description on the perspectives on the chemical micro-environments of Nafion films obtained in this thesis study.

References

[1] T. Xu, Ion exchange membranes: State of their development and perspective, J. Membr. Sci. 263 (2005) 1-29.

[2] J. Ran, L. Wu, Y. He, Z. Yang, Y. Wang, C. Jiang, L. Ge, Ion exchange membranes: New developments and applications, J. Membr. Sci. *522* (2017) 267-291.

[3] A. Kusoglu, A. Z. Weber, New Insights into Perfluorinated Sulfonic-Acid Ionomers, Chem. Rev 117 (2017) 987-1104.

Chapter 2

Review of the nature of fluoroalkyl chain and perfluorinated sulfonic-acid ionomers

2.1. Perfluoroalkyl chain chemistry

2.1.1. Fundamental nature of C-F bond

Various unique properties of fluorine compounds originate from the fluorine specific atomic physical properties. The fundamental fluorine substituent effect is reviewed by Smart [1] and O'Hagan [2]. Herein, their works are briefly summarized from viewpoints of atomic properties of fluorine and C-F bond properties. Additionally, the nature perfluoro alkyl (Rf) is described from new insight on C-F dipole direction.

The specific fluorine atomic properties are listed with those of halogens as reference elements in Table 2.1. The most notable fluorine property is the electronegativity. The Pauling electronegativity value of $\chi_p = 4$ is the highest value in all the elements. This specific property effects for various molecule properties; pKa change by inductive effect, thereby formed C-F bond provide unique properties. The Pauling electronegativity is defined as below [1]

$$E_{AB} = 1/2E_{AA} + 1/2E_{BB} + \Delta^2 \tag{2-1}$$

Where E_{AB} is the dissociation energy of A-B bond, E_{AA} and E_{BB} are the dissociation energies of two non-polar covalent bonds A-A and B-B are respectively, Δ is the difference in electronegativity between A and B. The value of $\chi_p = 4$ is originated from large energies of ionization potential and electronic affinity. Fluorine electron arrangement is ($1s^2$, $2s^2$, $2p^5$). Removal of an electron from a fluorine atom to generate F^+ is extremely difficult as the 2p electrons are held more closely by the nuclear charge. This fact corresponds to the large ionization potential of atomic fluorine. Simultaneously, the fluorine atom can readily accept an electron. The 2p orbital is filled by this electron, and thus the negative charge is stabilized

by the electro positive nuclear to greater extent than in more expanded valence orbitals with smaller nuclear charges such as those in oxygen with a much lower electro affinity.

Table 2-1. Atomic physical properties of halogen atoms. Taken from ref. [1]

	F	Cl	Br	I
I. P. (kcal/mol)	401.8	299.0	272.4	242.2
E. A. (kcal/mol)	79.5	83.3	72.6	70.6
χ_p (Pauling)	4.0	3.2	3.0	2.7
Van der Waals radius (r_v)	1.47	1.75	1.85	1.98

Additionally, fluorine has the second smallest van der waals radius after hydrogen. Fluorine substitution of hydrogen in organic compounds is often used for medical chemistry programs, because of the smallest steric effect. Fluorine substitution has significant electronic consequences and can dramatically change the properties of a molecule. In pharmacy, introducing of short Rf substituent group for medicant increase their contrasting binding selectivity, bioavailability, and metabolic stability in comparison with those of their alkyl analogues [3-5].

On the other hand, the steric effect of fluorinated effect exists. To illustrate this effect, the energies of non-bonded interactions between two hydrogen atoms, a hydrogen and a fluorine atom, and two fluorine atoms are plotted as a function of boundary distance as shown in Fig. 2-1. At 2.5 Å, there is negligible repulsion, i. e. no steric effect, but at 2.0 Å where there is considerable overlap effect. Examples of fluorine steric effects in two dynamic processes and a chemical reaction where fluorine substitution alters the normal trans-stereochemistry for addition of bromine to a double bond are given in Fig. 2-2. Furthermore, the most important steric effect of fluorine substitution is the

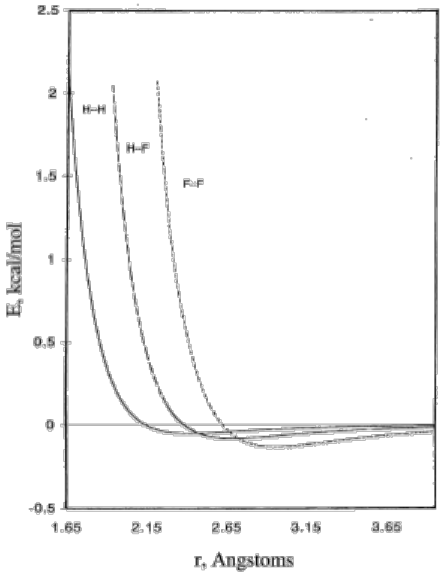

Fig. 2-1. van der Walls energies vs. inter-nuclear distances taken from ref. [1]

helical structure of per fluorination of carbon which affect Rf compounds properties as discussed in detail below.

The strongest electron negativity of fluorine largely effects the C-F bond property, and this bond properties largely effect for molecule properties. Table 2-2 shows bond properties of common covalent bonds. C-F bond has strongest bonding energy in the all covalent bond, and it bond strength affect the molecules properties which has C-F bond such as melting point, boiling point, chemical proof.

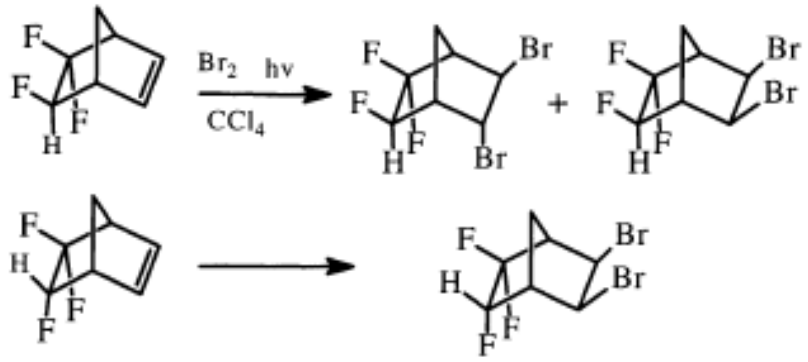

Fig. 2-2. Fluorine steric effect for product conformations. Taken from ref. [2]

Table 2-2. Bond length and Bond dissociation energy. Taken form ref. [2]

	C-H	**C-F**	C-O	C-C
Bond length / Å	1.09	1.35	1.43	1.54
Bond dissociation energy / kcal mol^{-1}	98.8	105.4	84.0	83.1

2.1.2 New insight of Rf compounds nature

In generally, perfluoro alkane is the substance which are substituted by fluorine. The prefix of “Per halogen” means all of hydrogen are substituted by the halogen element. The main-chain of polyethylene (alkyl chain) has planar zig-zag structure which in crystal region such as Fig. 2-3 (a), while polytetrafluoroethylene (PFTE, Rf chain polymer) has helical structure on the whole as shown in Fig. 2-3(b) [6]. The H···H atomic distance 2.534 Å is shorter than the sum of H···H van der waals radius 2.2 Å, there is no steric effect. Meanwhile,

The sum of F···F van der waals radius is 2.7 Å, these repulsion results in tortile structure. PTFE has 13 $(CF)_2$ units in a fiber period, and it twist 6 cycle under 19 ℃, these structure represented as (13/6). Over 19 ℃, it untwist and become (15/7) structure.

PTFE has very low relative permittivity and hydrophobic surface. However, considering strongly polarized C-F bond, it is more natural that considering Rf compound such as PTFE indicate hydrophilic and hydrophobic. Unveiling this irreconcilability of phenomenon and intuition lead to understanding, and these perceptions make newly application of Rf compounds. It is intriguingly that Hasegawa et al. challenge this theme [7], they analyzed Langmuir-Blodgett (LB) film of myristic acid and ratio changed fluorinated of alkyl chain of myristic acid. They modeled LB film of fluorinated mystic acid by surface pressure (π)-surface area (A) isotherms of the monolayer and IR reflection-absorption (RA) spectrometry. IR-RA spectrometry has adequately high sensitivity for measuring a monolayer.

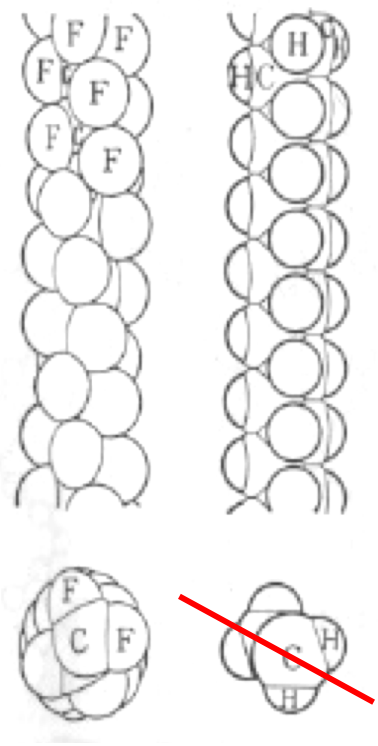

Fig. 2-3. Molecular structure models of (a) polytetrafluoroethylene (PTFE), (b) polyethylene. Taken from ref. [6]

Fig. 2-4 indicates myristic acid molecule model which fluorinated C9. The dipole of Rf $(CF)_2$ unit weaken by the dipole of contiguous Rf chain, bottom and top $(CF)_2$ units are not weakened due to tortile chain structure of Rf chain. Therefore, directions of these two dipoles is importance on evaluating formed LB film properties. These two dipoles is twisted 120° as shown as Fig. 2-4 (c). In Fig. 2-5, 2D-condensed film structure model divided by different Rf chain length of myristic acid molecules. In the case of under C6, molecule aggregation does not happen, it makes film which molecules lie on the water. From here onwards, molecules indicate inherent hydrophilic nature due to expose C-F bond dipoles. In the case of $(CF_2)_7$ molecule, tetragonal condensed structure which top and bottom dipoles orthogonalize. In the case of over C9, these dipoles is twisted 120° , molecules makes spontaneously hexagonal condensed structure, this film structure is the most stable film structure. The cross-sectional area ratio of tetragonal and

hexagonal structure is $(2/\sqrt{3}):1$. Hexagonal structure results in very low dielectric permittivity of long Rf chain compounds, because of which dipole moments are dispelled by each molecule. Additionally, the CF_3 terminal group which bond to electron poor CF_2 unit, it has properties close to tetrafluoromethane (CF_4). CF_4 is difficult solubility for water. Thus, Rf compounds which has hexagonal structure indicates hydrophobic surface. This is rationalized model which can explain the common nature of Rf compounds.

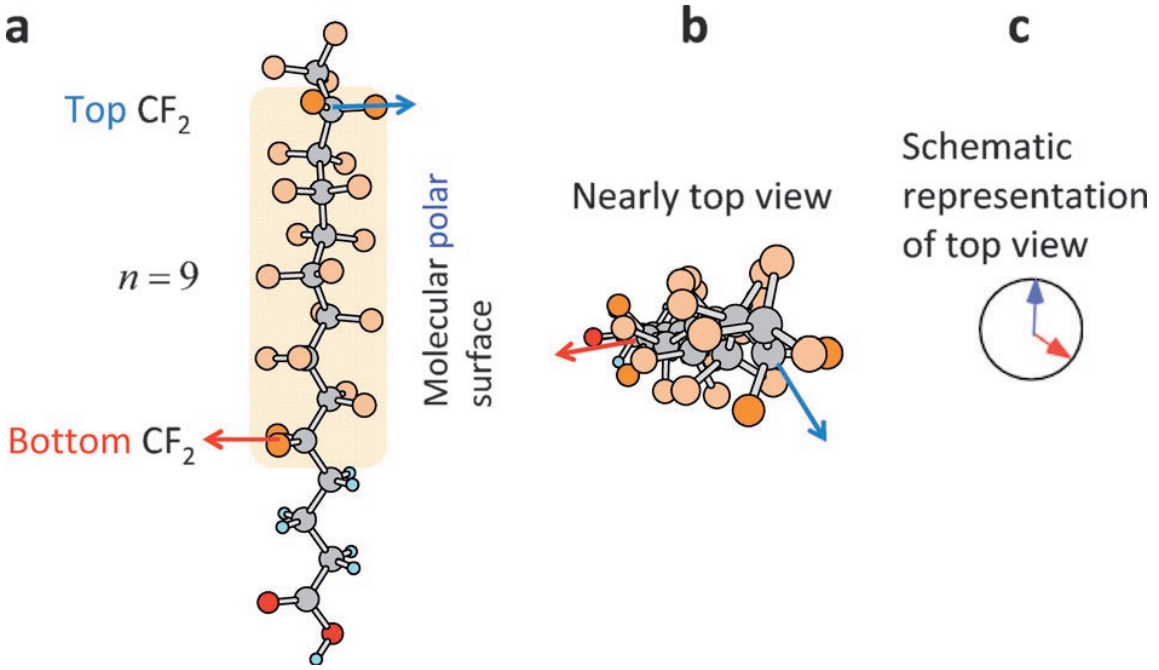

Fig. 2-4. Molecular structure models of (a) polytetrafluoroethylene (PTFE), (b) polyethylene. Taken from ref.[7]

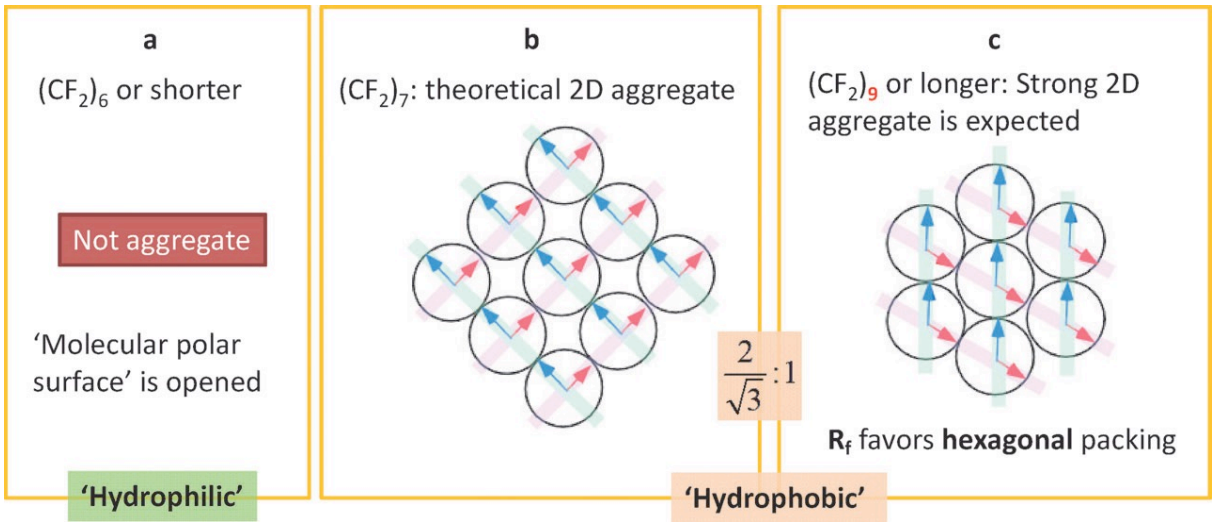

Fig. 2-5. Schematics of Stratified Dipole-Arrays theory depending of the Rf length. Taken from ref [7]

2.1.3. Short chain Rf

On the other hands, hydrophilicity of short Rf chain is newly revealed in a similar way. Short Rf chain is important for various scene such as pharmaceuticals, surfactant, surface preparation agent. For pharmaceutical, short Rf for their contrasting binding selectivity, bioavailability, and metabolic stability in comparison with those of their alkyl analogues [3-5]. Perfluoroalkyl surfactants show surface activity for both oil and water, but those with long Rf chains (over C8) are not biodegradable due to the high stability associated with the strong C-F bond; the resulting environmental consideration has motivated the development of short Rf chain surfactants [8].

2.2 Perfluoro sulfonated acid ionomers

2.2.1 Perfluoro sulfonated acid ionomers and its application

Proton transporting membranes have been among the fundamental materials supporting a variety of modern electrochemical devices and sensors. The most frequently used one is Nafion®. The Nafion films have found many applications for proton transportation [9], energy storage [10], energy conversion [11], catalytic reaction media [12], and in vivo measurements of neurotransmitter [13]. The electrochemical characteristics of the Nafion film and similar ionic polymer films as an ion exchange polymer membrane were originally described in the pioneering papers [14-16].

2.2.2. Nafion microstructure analysis using Spectroscopic method

A Nafion film immersed in water has a phase-separated structure composed of a micro water-phase and a perfluoroalkyl-phase. The water-phase is in a hydrophilic ionic channel as a micro water-domain surrounded by walls with condensed sulfonate groups of the side chains. The perfluoroalkyl-phase is a bulk region composed of perfluoroaklyl chains of Nafion. Because of the characteristic micro water-phase network structures, chemical micro-environment in a Nafion film has a specific electrostatic and hydrated nature. Studies based on the two-phase framework model with the water-phase and perfluoroalkyl-phase were extensively conducted through various approaches from a viewpoint of micro-structures of hydrated Nafion films. Using the results of spectroscopic measurements of hydrated Nafion

films by X-ray reflection and scattering and neutron-ray diffraction, a variety of nanoscopic and mesoscopic structure models have been proposed [17-23].

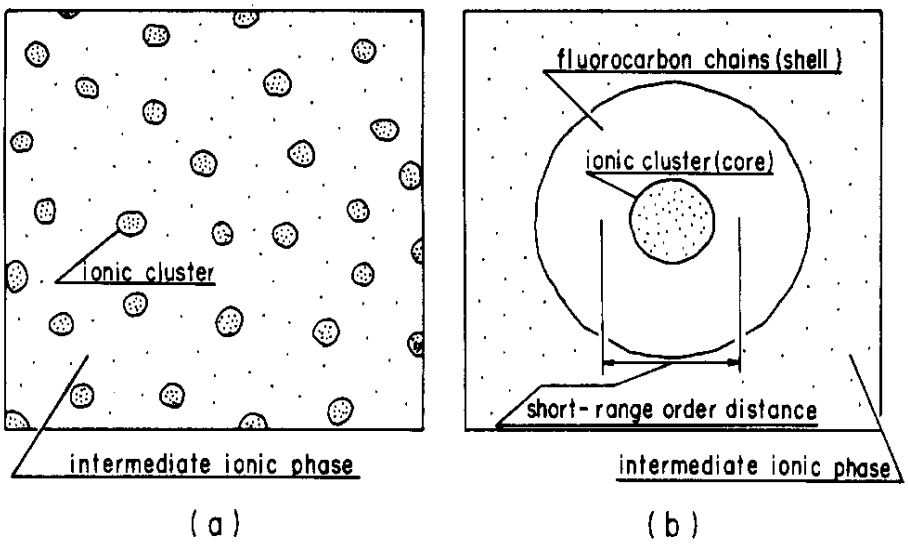

Fig. 2-6. Molecular structure models of (a) Two-phase model composed of ionic clusters, (b) polyethylene. Taken from ref.[17]

2.2.3. Nafion microstructure analysis using Molecular probe

The spectroscopic methods frequently have difficulty in gaining a better insight into the micro-phase structures in the hydrated Nafion films. On the other hand, analytical methods using molecule probes such as fluorescence probes [24-26], electron spin resonance probes [27], and redox probes [28,29] attain *in-situ* observation of chemical micro-environments in the hydrated Nafion films. Mortimer and Dillingham found Nafion's permeation allowance for dihexyl viologen and forbiddance for diheptyl viologen [30]. This fact confirms the known diameter of the channel, being smaller than 4.2 nm [31]. Viologen as a functional molecule is introduced into Nafion film formed on transparent SnO_2 electrode, and those diffusion constant [32] and the monomer-dimer equilibrium constant of the one-electron reduction [33] are measured by combined electrochemical-spectrophotometric Method. Fig. 2-7 shows used three types of viologen that has different total charge, and Table 2-3 shows measured those diffusion coefficients of oxidant form in Nafion. The three types of viologen indicate close values in lower concentration, but those have different concentration dependences. As seen

from the above, signals form molecule probe in Nafion analyzing is effective method for obtaining Nafion micro structure and chemical environment information.

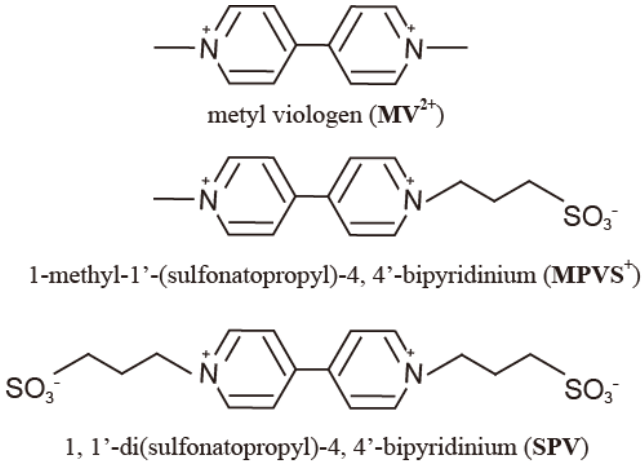

Fig. 2-7. Structure formula of Three type viologen Methyl viologen (**MV^{2+}**), 1-methyl-1'-(sufonatopropyl)-4, 4'-bipyridinium (**$MPVS^{+}$**) 1,1'-di(sulfonatopropyl)-4,4'-bipyridinium (**SPV**). Taken from ref.[32]

Table 2-3. Apparent Diffusion Coefficients of Three Viologens. Taken from ref. [32]

	Concn in Nafion, M	$10^9 D^a$ $cm^2 s^{-1}$	$10^9 D^b$ $cm^2 s^{-1}$
MV_2^+	0.12	8.0	
	0.23	7.7	7.0
	0.45	3.5	
	0.65	1.8	
$MPVS^+$	0.12	10	
	0.18	10	7.0
	0.27	5.0	2.5
	0.64	4.2	
SPV	0.12	8.0	6.0
	0.30	1.5	

[a]By spectrophotometric measurements at 550 mm; thickness of films (1.8-2.3) * 10^{-4} cm. [b]By cyclic voltammetry.

2.2.4. Microstructure of Nafion/substrate interface

A solid/Nafion interfacial structure depends on the chemical nature of the substrate. For example, on the silicon oxide (SiO_2) hydrophilic surface, a neutron reflectometry approach to a hydrated Nafion film by Dura and co-workers found lamellae composed of interlaminated thin water-rich and fluoroalkyl phase layers [34]. The lamellae are thicker and more in number at higher humidity, whereas such a multilayer structure was not formed on a Au or Pt surface as shown in Fig 2-8. At Au and Pt electrode surfaces, potential-dependent adsorption and desorption processes of a perfluorosulfonated ionomer, the constituent element of Nafion, were monitored by Masuda and co-workers [35]. His group also reported the strong adsorption of the ionomer on a Au(1 1 1) electrode in acidic condition by contacting sulfonated groups to the Au surface in the potential range from 0.0 V to 1.0 V (Ag/AgCl) [36]. An atomic force microscopic approach coupled with an electrochemical technique by Ohira and colleagues unveiled that the presence, abundance, and connectivity of water-filled proton conducting channels in Nafion films sharply depend on their 10 nm-level total thickness as well as underlying solid-substrate surface chemistry [37].

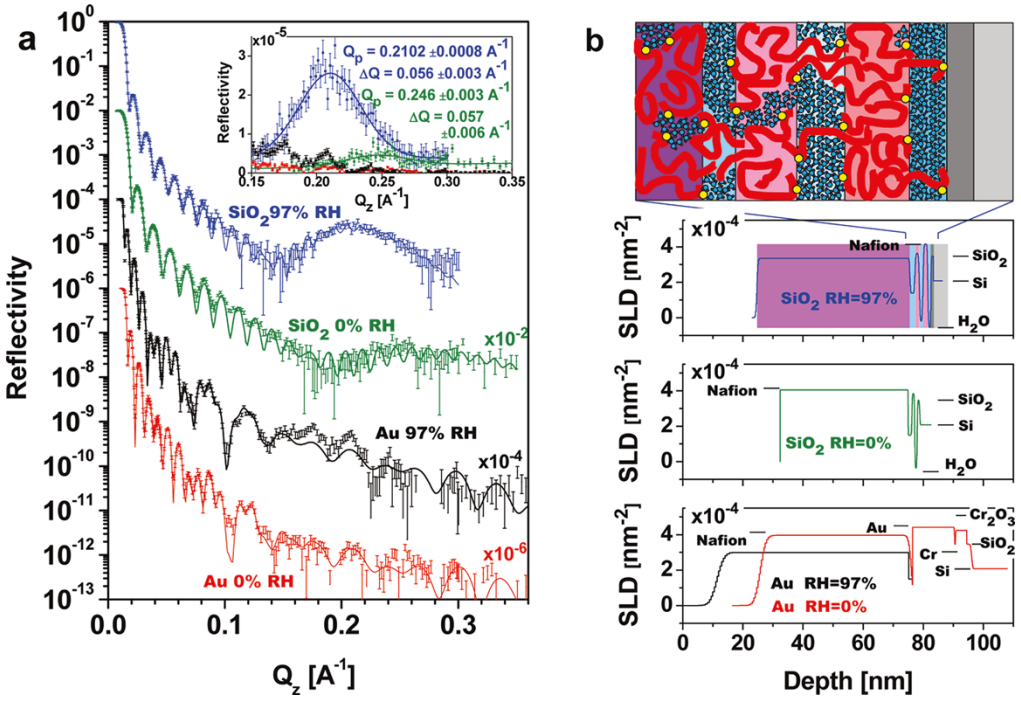

Fig. 2-8. Specular neutron reflectivity data, fits, and models for Nafion on SiO_2 and Au. (a) Specular neutron reflectivity data and model fits showing a high-Q peak for SiO_2 at RH=97% (blue) and a smaller high-Q peak for SiO_2 at RH=0% (green), whereas no high-Q peak for Au with RH=97%(black) or for Au at RH=0 (red) is observed. (b) SLD profiles corresponding to the four fits in (a). An artist's rendition (not to scale) of the model corresponding to SiO_2-60 at RH=97%is shown above its SLD profile with the Nafion fluorocarbon backbone in red, sulfonic acid in yellow, and water in blue. Taken from ref. [34]

2.2.5. Control of Nafion/substrate interface by underling monolayer

The question how the pre-modification of the electrode surface by an organic ultra-thin film before casting the Nafion affects the interfacial structure is not well answered up to now. The molecular-level regulation of the Nafion/substrate interface is expected as a promising mean to optimize the electron and proton transfer processes as well as film micro-structures. Establishment of such a double layer modification technique for Nafion may provide us with a wealth of opportunities to regulate the interfacial behavior on an electrode and catalyst, whereas the reports on the technique are presently limited.

Modestino and coworkers compared the nano-structure of a Nafion thin-film on a native oxidized Si surface to that on a *n*-octyltrichlorosilane (OTS) passivated Si substrate using a grazing-incidence small-angle X-ray scattering technique [38]. They detected an isotropic orientation of ion-channels on the SiO_2 surface on Si and a parallel orientation of the channels on the hydrophobic OTS-passivated Si surface. The difference gave sharp contrast in their water uptake processes from the external humidified environments: the uptake was retarded on the OTS-passivated Si substrate as shown in Fig 2-9. Cha and colleagues used an alkanethiol self-assembled monolayer (SAM) on a Au electrode to reinforce the adhesion of the Nafion film to the electrode [39]. When using a dodecane thiol SAM, they confirmed validness to gain stronger adhesion and durability without degradation of the redox response of cationic species across the Nafion film. After their work, we cannot find any report describing the metal electrode/SAM/Nafion structure, and thus the merits and problems to insert such an organic monolayer in between metal and Nafion have been left unanswered.

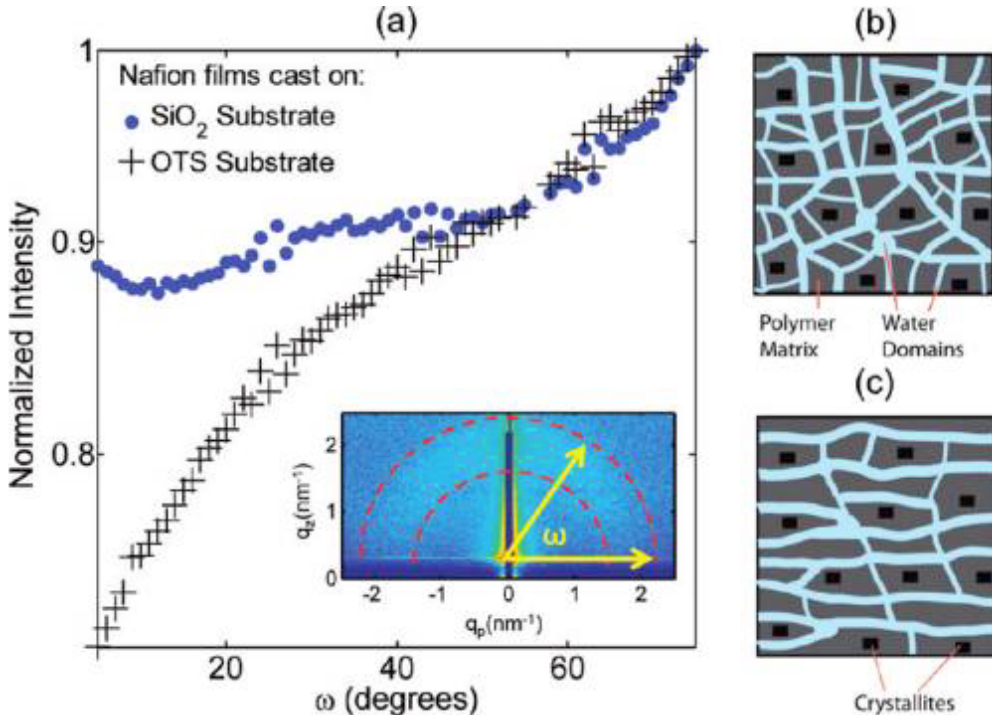

Fig. 2-9. (a) Ionomer peak intensity for films cast on SiO_2 and OTS as a function of orientation angle (ω) at early stages of swelling. The inset shows the ionomer peak region selected for the integration of scattering intensity. Higher levels of anisotropy are observed for films cast on OTS, suggesting a larger distribution of ionomer channels oriented parallel to the substrate when compared to films cast on Si. The general schematic of ionomer thin film morphology in (b) and (c) correspond to representations of ionomer channel distribution for films cast on Si and OTS passivated substrates, respectively. Taken from ref. [38]

References (Chap. 2)

[1] Smart, B. E., Fluorine substituent effects (on bioactivity). J. Fluorine Chem. 109 (2001) 3-11.

[2] O'Hagan, D., Understanding organofluorine chemistry. An introduction to the C–F bond. Chem. Soc. Rev. 37 (2008) 308-319.

[3] M. Shimizu, T. Hiyama, Modern Synthetic Methods for Fluorine-Substituted Target Molecules, Angew. Chem. Int. Ed. 44 (2) (2005) 214-231.

[4] J. Wang, M. Sánchez-Roselló, J. L. Aceña, C. del Pozo, A. E. Sorochinsky, S. Fustero, V. A. Soloshonok, H. Liu, Fluorine in Pharmaceutical Industry: Fluorine-Containing Drugs Introduced to the Market in the Last Decade (2001−2011), Adv. Mater. 114 (4) (2014) 2432-2506.

[5] X. Shao, C. Xu, L. Lu, Q. Shen, Shelf-Stable Electrophilic Reagents for Trifluoromethylthiolation, Acc. Chem. Res 48 (5) (2015) 1227-1236.

[6] S. Murahashi, H. Hujita, S. Nozakura: Koubunnshikagaku third edition, Kyoritsu shuppan (1983)

[7] T. Hasegawa, Physicochemical Nature of Perfluoroalkyl Compounds Induced by Fluorine, Chem. Rec. 17 (10) (2017) 903-917.

[8] E. Kang, G. Y. Jung, S. H. Jung, B. M. Lee, Synthesis and surface active properties of novel anionic surfactants with two short fluoroalkyl groups, J. Ind. Eng. Chem. 61 (2018) 216–226

[9] P. Choi, N.H. Jalani, R. Datta, Thermodynamics and Proton Transport in Nafion II. Proton Diffusion Mechanisms and Conductivity, J. Electrochem. Soc. 152 (3) (2005) E123-E130.

[10] F. Lufrano, P. Staiti, Performance improvement of Nafion based solid state electrochemical supercapacitor, Electrochim. Acta 49 (15) (2004) 2683-2689.

[11] X.-L. Zheng, J.-P. Song, T. Ling, Z.P. Hu, P.-F. Yin, K. Davey, X.-W. Du, S-.Z. Qiao, Strongly Coupled Nafion on Molecules and Ordered Porous CdS Networks for Enhanced Visible-Light Photoelectrochemical Hydrogen Evolution, Adv. Mater. 28 (24) (2016) 4935-4942.

[12] S.M. Jain, S. Tripathi, S. Tripathi, G. Spoto, T. Edvinsson, Acid-catalyzed Oligomerization via Activated Proton Transfer to Aromatic and Unsaturated Monomers in Nafion Membranes: A step forward in the in situ synthesis of Conjugated Composite Membranes, RSC Advances 6 (2016) 104782-104792.

[13] M. W. Espenscheid, A. R. Ghatak-Roy, R. B. Moore, III, R. M. Penner, M. N. Szentirmay, C. R. Martin, Sensors from Polymer Modified Electrodes, J. Chem. Soc., Faraday Trans. 82 (1) (1986) 1051-1070.

[14] N. Oyama, T. Shimomura, K. Shigehara, F. C. Anson, Electrochemical Responses of Multiply-Charged Transition Metal Complexes Bound Electrostatically to Graphite Electrode Surfaces Coated with Polyelectrolytes, J. Electroanal. Chem. 112 (1980) 271-280.

[15] I. Rubinstein, A. J. Bard, Polymer Films on Electrodes. 4. Nafion-Coated Electrodes and Electrogenerated Chemiluminescence of Surface-Attached $Ru(bpy)_3^{2+}$, J. Am. Chem. Soc. 102 (1980) 6641-6642

[16] P. Ugo, L. M. Moretto, Ion-Exchange Voltammetry at Polymer-Coated Electrodes: Principles and Analytical Prospects, Electroanalysis 7 (12) (1995) 1105-1113.

[17] M. Fujimura, T. Hashimoto, H. Kawai, Small-Angle X-ray Scattering Study of Perfluorinated Ionomer Membranes. 1. Origin of Two Scattering Maxima, Macromolecules 14 (5) (1981) 1309-1315.

[18] W.Y. Hsu, T. Gierke, Ion transport and clustering in Nafion perfluorinated membranes, J. Membr. Sci. 13 (3) (1983) 307-326.

[19] G. Gebel, Structural evolution of water swollen perfluorosulfonated ionomers from dry membrane to solution, Polymer 41 (15) (2000) 5829-5838.

[20] H.-G. Haubold, Th. Vad, H. Jungbluth, P. Hiller, Nano structure of NAFION: a SAXS study, Electrochim. Acta 46 (10-11) (2001) 1559-1563.

[21] L. Rubatat , A.L. Rollet , G. Gebel , O. Diat, Evidence of Elongated Polymeric Aggregates in Nafion, Macromolecules 35 (10) (2002) 4050-4055.

[22] K.S. Rohr, Q. Chen, Parallel cylindrical water nanochannels in Nafion fuel-cell membranes, Nat. Mater. 7 (2008) 85-83.

[23] K. D. Kreuer, G. Portale, A Critical Revision of the Nano-Morphology of Proton Conducting Ionomers and Polyelectrolytes for Fuel Cell Applications, Adv. Funct. Mater. 23 (43) (2013) 5390-5397.

[24] X.-Y. Yi, L.-Z. Wu, C.-H. Tung, Long-Lived Photoinduced Charge Separation in $Ru(Bpy)_3^{2+}$/Viologen System at Nafion Membrane-Solution Interface, J. Phys. Chem. B, 104 (40) (2000) 9468-9474.

[25] Y.P. Patil, T.A. P. Seery, M.T. Shaw, R.S. Parnas, In Situ Water Sensing in a Nafion Membrane by Fluorescence Spectroscopy, Ind. Eng. Chem. Res., 44 (16) (2005) 6141-6147.

[26] L.M. Moretto, T. Kohls, A. Chovin, N. Sojic, P. Ugo, Epifluorescence Imaging of Electrochemically Switchable Langmuir-Blodgett Films of Nafion, Langmuir, 24 (12) (2008) 6367-6374.

[27] T. Überrück, O. Neudert, K. Kreuerd, B. Blümich, J. Granwehr, S. Stapf, S. Han, Effect of nitroxide spin probes on transport properties in Nafion membranes, Phys. Chem. Chem. Phys., 41(20) (2018) 26660-26674.

[28] M. Shi, F.C. Anson, Some Consequences of the Significantly Different Mobilities of Hydrophilic and Hydrophobic Metal Complexes in Perfluorosulfonated Ionomer Coatings on Electrodes, Anal. Chem., 69 (14) (1997) 2653-2660.

[29] A. Yamauchi, Kazuki Togami, Ashraf M. Chaudryb, A. Mounir EL Sayed, Characterization of charged film of fluorocarbon polymer (Nafion) and blended fluorocarbon polymer (Nafion)/Collodion composite membranes by electrochemical methods in the presence of redox substances. V, J. Membrane Sci. 249 (1-2) (2005) 119-126.

[30] R. J. Mortimer, J. L. Dillingham, Electrochromic 1,1'-Dialkyl-4,4'-bipyridilium-Incorporated Nafion Electrodes, J. Electrochem. Soc. 144 (5) (1997) 1549-1553.

[31] S. Shia, A. Z. Webera, A. Kusoglu, Stracture-transport relationship of perfluorosulfonic-acid membranes in different cationic forms, Electrochim. Acta 220 (1) (2016) 517-528.

[32] A.M. Hodges, O. Johansen, J.W. Loder, A.W. H. Mau, J. Rabani, W. H. F. Sasse, Diffusion of viologens in Nafion film studied by a combined electrochemical-spectrophotometric method, J. Phys. Chem. 95(15) (1991) 5966-5970.

[33] O. Johansen, J. W. Loder, A. W. H. Mau, J. Rabani, W. H. F. Sasse, Properties of reduced viologens in Nafion films deposited on tin dioxide electrodes, Langmuir 8 (10) (1992) 2577-2581.

[34] J. A. Dura, V. S. Murthi, M. Hartman, S. K. Satija, and C. F. Majkrzak, , Multilamellar Interface Structures in Nafion, Macromolecules 42 (13) (2009) 4769-4774.

[35] T. Masuda, F. Sonsudin, P. R. Singh, H. Naohara, and K. Uosaki, Potential-Dependent Adsorption and Desorption of Perfluorosulfonated Ionomer on a Platinum Electrode Surface Probed by Electrochemical Quartz Crystal Microbalance and Atomic Force Microscopy, J. Phys. Chem. C 117 (30) (2009) 15704-15709

[36] T. Masuda, K. Ikeda, and K. Uosaki, Potential-Dependent Adsorption/Desorption Behavior of Perfluorosulfonated Ionomer on a Gold Electrode Surface Studied by Cyclic Voltammetry, Electrochemical Quartz Microbalance, and Electrochemical Atomic Force Microscopy, Langmuir 29 (7) (2013) 2420-2426

[37] A. Ohira, S. Kuroda, H. F. M. Mohamed, and B. Tavernierb, Effect of interface on surface morphology and proton conduction of polymer electrolyte thin films, Phys. Chem. Chem. Phys. 15 (2013) 11494-11500

[38] M. A. Modestino, A. Kusoglu, A. Hexemer, A. Z. Weber, and R. A. Segalman, Controlling Nafion Structure and Properties via Wetting Interactions, Macromolecules 45 (11) (2012) 4681–4688

[39] C. S. Cha, J. Chen, and P. F. Liu, Improvement of the adhesion of a Nafion® modifying layer on electrodes, J. Electroanal. Chem. 345 (1-2) (1993) 463-467

Chapter 3

Experimental Methodology

A description of the materials, experimental techniques, instruments and brief outline of the electroreflectance (ER) spectroscopic used for data collection are presented in this chapter.

3.1. Materials

Water was purified through a Milli-Q Plus Ultrapure water system coupled with an Elix-5 kit (Millipore Co.) to 18.2 MΩ cm. Materials used without further purification include 4,4'-bipyridine (TCI), 1,1,1,2,2-pentafluoro-4-iodobutane (Sigma Aldrich), Nafion 5 wt.% solution (Sigma Aldrich), KCl (Nacalai Tesque), KPF_6 (Sigma Aldrich), tetrabutylammonium chloride (TCI), 1-decanethiol (Sigma-Aldrich), ω-hydroxy-hexanethiol (Sigma-Aldrich) and *1H,1H,2H,2H*-perfluoro-1-octanedecanethiol (Sigma-Aldrich), diethyl ether (EP grade, Nacalai Tesque), acetone (HPLC grade, Nacalai Tesque), and ethanol (HPLC grade, Nacalai Tesque). All other chemicals were of the highest reagent grade commercially available and used as received.

3.2. Synthesis

1,1,1,2,2-Pentafluoro-4-iodobutane (1.70 mmol) was added in *N,N*'-dimethylformamide (DMF) solution of 4,4'-bipyridine (0.71 mmol) at 100°C. After 24 h stirring, orange precipitate was collected by filtration as the crude product. It was washed by diethyl ether and acetone and dried over silica gel in a desiccator. The counter anion iodide of the product was exchanged for chloride using an anion exchange resin, Amberlite IR-400. Recrystallization of white chloride salt from ethanol gave a layered crystal of *N,N'*-di-1*H*,1*H*,2*H*,2*H*-perfluorobutyl-4,4'-bipyridinium dichloride (FC4VFC4 in scheme 1) with a yield of 28.2 %. It was characterized by ^{1}H NMR, ^{19}F NMR, and FAB-MS. All the details are listed here: ^{1}H NMR (300 MHz, DMSO-d6, TMS ref.): δ = 3.23 (m, 4H), 5.09 (t, 4H), 8.89 (d, 4H), 9.51 (d, 4H); ^{19}F NMR (400 MHz, DMSO-d6, HFB ref.): δ = 87.13 (s, 4F), 118.58 (t, 4F); and FAB-MS: m/z calc. for $[(\text{deprotonated } M^{2+})Cl_2]^-$ 520.23, found 520.2.

N,N'-dibutyl viologen dichloride (C4VC4 in scheme 1), synthesized through the Menshutkin reaction of 4,4'-bipyridine with 1-bromobutane, was subjected to counter anion

exchange from iodide to hexafluorophosphate and then to chloride. Home-synthesized methyl viologen dichloride ($MV^{2+}Cl^{-}_{2}$) was also used as a reference compound.

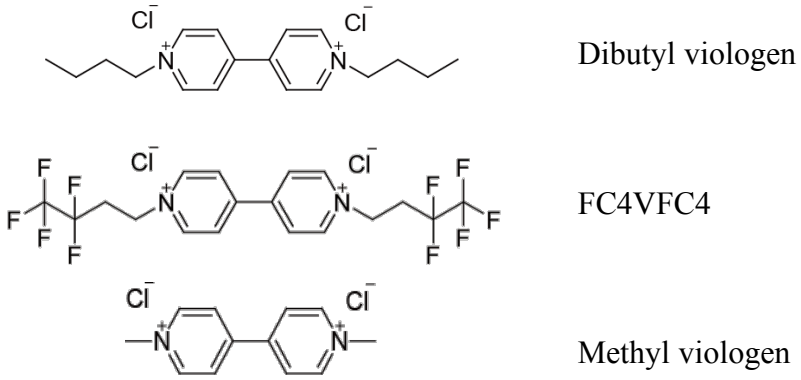

Scheme 1. Viologen derivatives as chloride salts

3.3. Electrochemical and Electroreflectance (ER) Measurements

All the electrochemical measurements were conducted using either polycrystalline Au electrode with a surface area of 0.021 cm^2 (BAS Inc.) with a PEEK sheath or an ultra-micro Au electrode (surface area, 74.97 μm^2, BAS Inc.) with a glass sheath. Voltammetric studies were conducted using a Ag|AgCl|sat'd KCl reference electrode and a coiled Au wire counter electrode. All the potentials in this paper are referenced to a Ag|AgCl|sat'd KCl. All the measurements were performed under an Ar gas (> 99.998%) atmosphere at room temperature (25 ± 2°C).

For the voltammetric measurements, a potentiostat (HECS 326, HUSOU) was employed. The base electrolyte solution in electrochemical measurements was 0.1 M KCl solution unless otherwise stated. Voltammetric studies at the ultra-micro Au electrode (Au-UME) were conducted using a nA-unit head box (HUSOU 972-1).

The electrochemical behaviors of viologens were characterized at bare and Nafion-modified electrodes. The coating of the Au electrode surface with a Nafion film was conducted by casting 10 μL of 0.5 wt% Nafion solution homogeneously on both the centered Au and surrounding PEEK coplanar circular surface (in total 0.283 cm^2). The solvent used to dilute as-purchased Nafion solution was isopropane. It was then dried in air. The thickness of the dry Nafion film on the Au surface was 1.0 ± 0.2 μm as measured by a scratching method

of a contact mode AFM imaging. Before use, the Nafion film on the electrode was swelled by immersing the electrode in the supporting electrolyte solution free of viologen.

For the electrochemical measurements, a potentiostat (HECS 326, HUSOU) was employed. The base electrolyte solution in electrochemical measurements was 0.1 M KCl solution unless otherwise stated. For the time-course measurements of cyclic voltammograms (CVs), the time zero was set when the Nafion modified Au electrode was immersed in a pre-deaerated viologen solution in the electrochemical cell. At certain times, a single potential-cycle CV recording was made at a scan rate (v) of 200 mV s^{-1}.

The potential modulation used for the ER measurements is described as

$$E = E_{dc} + E_{ac} = E_{dc} + \Delta E_{ac}\exp(j\omega t) \qquad [3\text{-}1]$$

where E_{dc} is the dc potential, E_{ac} is the ac potential, ΔE_{ac} is the zero-to-peak ac amplitude of the potential modulation, $j = \sqrt{-1}$, $\omega = 2\pi f$, where f is the modulation frequency, and t is the time. The instruments and procedures used for the ER measurements were described elsewhere [1]. Briefly, under the ac potential modulation, steady-state monochromatic light was irradiated to the electrode surface. The reflected light was detected by a photomultiplier (Hamamatsu R928) to analyze ac reflectance signal using a lock-in amplifier (EG&G, model 5210). The time-averaged dc reflectance, R_{dc}, was also monitored simultaneously. Normalization of the ac signal by R_{dc} gave the real part ER signal $(\Delta R/R)_{real}$ (in-phase component with respect to E_{ac}) and the imaginary part $(\Delta R/R)_{imag}$ (90° out-of-phase component). If the reflectance change follows E_{ac} without any delay, $(\Delta R/R)_{imag}$ should be zero. The delay may originate from the electron-transfer kinetics as well as the nonzero cell time constant determined by the double-layer capacitance and bulk resistance.

The used program for the combined ER and CV measurements was a train setting shown in Scheme 2. All the ER and CV were recorded until reaching saturation of CV. The scanned wavelength region was restricted to a narrow range, from 640 to 440 nm, to minimize condition change during the wavelength scan. The E_{dc} for each ER spectral measurement was

set at E_m read from the immediately preceding CV chart, where E_m is the midpoint potential of anodic and cathodic peaks of viologen redox.

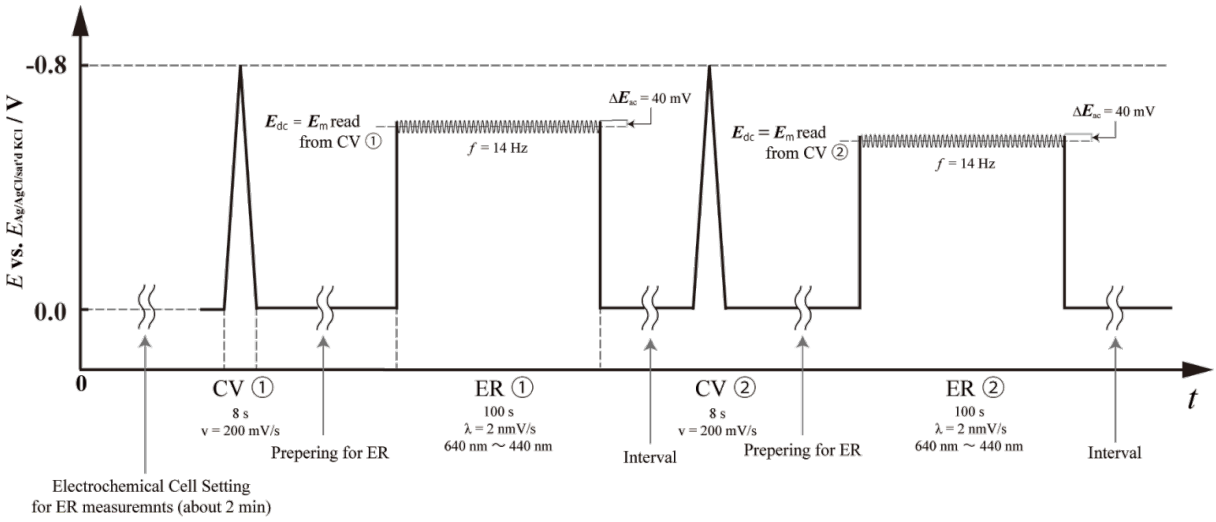

Scheme 2. Program used for combined ER and CV time-course measurements, showing applied potential as a function of time. The time zero corresponds to the immersion of the Nafion-coated electrode in 50 μM viologen + 0.1 M KCl solution. For ER, ΔE_{ac} = 56.4 mV and f = 14 Hz.

3.4. Quantum chemistry computations

Standard density functional theory (DFT) computations were carried out with Gaussian 16 [2]. Geometry optimizations and harmonic vibrational frequency calculations were carried out using the N12 method [3] in conjunction with the 6-31G(d) basis set. Improved single-point energies were calculated with the MN15 functional [4] and the 6-311+G(3df,2p) basis set. Zero-point vibrational energies, thermal corrections to 298 K enthalpies, and 298 K entropies were obtained using N12/6-31(d) frequencies scaled by previously determined scale factors [5]. The effect of aqueous solvation was incorporated using the SMD continuum solvation model [6] using densities calculated with the M05-2X functional [7] together with the 6-31G(d) basis set. Relative energies are reported in kJ mol^{-1}.

References (Chap. 3)

[1] A. Yamauchi, Kazuki Togami, Ashraf M. Chaudryb, A. Mounir EL Sayed, Characterization of charged film of fluorocarbon polymer (Nafion) and blended fluorocarbon polymer (Nafion)/Collodion composite membranes by electrochemical methods in the presence of redox substances. V, J. Membrane Sci. 249 (1-2) (2005) 119-126.

[2] M. J. Frisch, G. W. Trucks, H. B. Schlegel, G. E. Scuseria, M. A. Robb, J. R. Cheeseman, G. Scalmani, V. Barone, G. A. Petersson, H. Nakatsuji, X. Li, M. Caricato, A. V. Marenich, J. Bloino, B. G. Janesko, R. Gomperts, B. Mennucci, H. P. Hratchian, J. V. Ortiz, A. F. Izmaylov, J. L. Sonnenberg, D. Williams-Young, F. Ding, F. Lipparini, F. Egidi, J. Goings, B. Peng, A. Petrone, T. Henderson, D. Ranasinghe, V. G. Zakrzewski, J. Gao, N. Rega, G. Zheng, W. Liang, M. Hada, M. Ehara, K. Toyota, R. Fukuda, J. Hasegawa, M. Ishida,T. Nakajima, Y. Honda, O. Kitao, H. Nakai, T. Vreven, K. Throssell, J. A., Jr. Montgomery, J. E. Peralta, F. Ogliaro, M. J. Bearpark, J. J. Heyd, E. N. Brothers, K. N. Kudin,; V. N. Staroverov, T. A. Keith, R. Kobayashi, J. Normand,; K. Raghavachari, A. P. Rendell, J. C. Burant, S. S. Iyengar, J. Tomasi, M. Cossi, J. M. Millam, M. Klene, C. Adamo, R. Cammi, J. W. Ochterski, R. L. Martin, K. Morokuma, O. Farkas, J. B. Foresman, D. J. Fox, Gaussian 16 Revision B.01, Gaussian, Inc., Wallingford, CT, 2016.

[3] R. Peverati, D. G. Truhlar, Exchange-Correlation Functional with Good Accuracy for Both Structural and Energetic Properties while Depending Only on the Density and Its Gradient, J. Chem. Theory Comput. 7 (8) (2012) 2310-2319.

[4] H. S. Yu, X. He, S. L. Li, D. G. Truhlar, MN15: A Kohn-Sham Global-Hybrid Exchange-Correlation Density Functional with Broad Accuracy for Multi-Reference and Single-Reference Systems and Noncovalent Interactions, Chem. Sci. 7 (8) (2016) 5032-5051.

[5] B. Chan, Use of Low-Cost Quantum Chemistry Procedures for Geometry Optimization and Vibrational Frequency Calculations: Determination of Frequency Scale Factors and Application to Reactions of Large Systems, J. Chem. Theory Comput. 12 (13) (2017) 6052-6060.

[6] A. V. Marenich, C. J. Cramer, D. G. Truhlar, Universal Solvation Model Based on Solute Electron Density and a Continuum Model of the Solvent Defined by the Bulk Dielectric Constant and Atomic Surface Tensions, J. Phys. Chem. B 18 (113) (2009) 6378-6396.

[7] Y. Zhao, N. E. Schultz, D. G. Truhlar, Design of Density Functionals by Combining the Method of Constraint Satisfaction with Parametrization for Thermochemistry, Thermochemical Kinetics, and Noncovalent Interactions, J. Chem. Theory Comput. 2 (2) (2006) 364-382.

Chapter 4

Fluorination effect on electrochemistry of dibutyl viologen in aqueous solution

ABSTRACT. We explored the electrochemistry of a newly synthesized perfluoroalkyl viologen, *N*,*N*'-di-(1*H*,1*H*,2*H*,2*H*-perfluorobutyl)-4,4'-bipyridinium dichloride (FC4VFC4), in an aqueous solution and in a Nafion film on an Au electrode. The aim was to develop a redox-active probe for chemical micro-environments of the separated phases in the Nafion film. Aqueous solution electrochemistry of FC4VFC4 was described using the results of voltammetric measurements at a bare Au electrode, referring to dibutyl viologen. The time course of cyclic voltammograms was tracked after immersion of a Nafion film-modified Au electrode in the solution of FC4VFC4. The sharply concentration-dependent time change revealed the formation of an aggregate of FC4VFC4 in the ionic channels in Nafion; the aggregate blocks its own redox reaction at higher solution concentrations than 10 μM. In contrast, dibutyl viologen showed a quasi-reversible response at the same concentration. At 5 μM, FC4VFC4 clearly exhibited a quasi-reversible electrochemical response in the Nafion film. These results suggest that, when the concentration of FCVFC4 in ionic channels in the Nafion is over a critical concentration, FC4VFC4 accumulates there as a salt formed with anion sites on the channel inner wall with a help of perfluoroalkyl chain-chain interaction. The chain-chain interaction may include intermolecular one and the one between FCVFC4 and perfluoro- or boundary-phase.

4.1. Introduction

Redox reactions of organic electroactive species can be highly sensitive to the micro-environment. If neither a proton transfer nor a counter ion binding accompanies the electron transfer process, the redox reaction is governed by properties of the medium. We can, therefore, use such an electroactive molecule as a probe for the medium. We may probe the chemical micro-environments in organic and inorganic thin films, ionic liquids, metal-organic frameworks, and molecular-assembled structures that are yet to be clarified. Among the most widely used redox cores of the probes are ferrocene and viologen derivatives [1]. As far as their one-electron transfer reactions are concerned, one or both of the oxidation states of the aromatic redox cores, ferrocenyl and 4,4'-bipyridilium groups, are cationic and show π- π and electrostatic interactions with surrounding molecules. These oxidation-sate dependent interactions are also affected by substituents such as side-chain groups. A deeper understanding of the various contributing factors to these interactions would facilitate finer tuning of the redox probe.

In this work, we use viologen to examine the effect of Rf chain on physicochemical characteristics. This choice is based on the specific and desirable properties of viologen such as its reversible and stable one-electron redox activity that are associated with distinct color change. The one-electron reduction product of a viologen dication (V^{2+}), i.e., $V^{\bullet+}$, has a strong tendency to form a π-stacked dimer $(V^{\bullet+})_2$. The distinct color differences between V^{2+}, $V^{\bullet+}$, and $(V^{\bullet+})_2$ enables the use of UV-visible spectroelectrochemical methods for analysis. When a Rf-chain forms a part of the viologen, it can act as a local probe for, in addition to electrostatic interactions, dipole-dipole attractive interaction between C-F bonds, such as those occuring in perfluorinated anionic surfactant. Our interest lies also in how efficiently a Rf group can withdraw electron from the rather electron-deficient cationic viologen core.

Specifically, we synthesized a new perfluoalkyl viologen, *N*,*N*'-di-(1*H*,1*H*,2*H*,2*H*-perfluorobutyl)-4,4'-bipyridinium dichloride (FC4VFC4), as shown in Scheme 1, and compare the electrochemistry of this Rf-bearing *water-soluble* viologen with that of the analogous alkyl-bearing viologen counterpart. Water-solubility is a crucial characteristic of this molecule such that it can approach water/oil interface from the aqueous phase. This in turn enables us in future work to use it as a probe for inter-domain environment of a

phase-separated polymer such as a Nafion membrane. Singh and Shreeve have synthesized a series of viologen compounds with longer fluoroalkyl chains [2]; however, even their shortest-chain molecule, FC8VFC8, was sparingly soluble in water, precluding aqueous electrochemical characterization. Previously, we synthesized FC6VFC6 diiodide but we found that it is insoluble in water.

We have conducted electrochemical measurements for FC4VFC4 in an aqueous solution at a Au electrode. We focus on the one-electron transfer process of the $V^{\bullet+/}V^{2+}$ redox couple. We report herein the results of electrochemical measurements at a bare macro Au electrode and an ultra-micro Au electrode in a bulk aqueous medium, as well as insights obtained from out DFT computations.

4.2 Result and Discussion

4.2.1. Voltammetric Studies at macro-Au electrode

First, the results of voltammetric measurements were used to describe the electrochemistry of FC4VFC4 in aqueous solution in comparison with that of C4VC4. CVs of a bare 0.021 cm^2-Au electrode in 0.5 mM C4VC4 are shown in Fig. 4-1-a and those for FC4VFC4 in Fig. 4-1-b. A redox peak pair originated from the solution phase $V^{\bullet+/2+}$ couple for both viologens. The midpoint potential (E_m) between the anodic peak potential (E_{pa}) and the cathodic one (E_{pc}) at v = 100 mV s^{-1} was equated to the formal potential, $E^{o'}$, which was -648 and -518 mV for C4VC4 and FC4VFC4, respectively.

Because of the occurrence of electro-catalytic reduction of residual oxygen even after being purged by Ar gas, small additional cathodic current appeared at around -0.3 V. We did not take further efforts to remove oxygen, because this level of cathodic current never affected our analysis of the solution phase redox of viologens. The peak separation, ΔE_p, for C4VC4 was constantly 61 mV in the range of v varied from 10 to 200 mV s^{-1}. In contrast, the ΔE_p for FC4VFC4 was 66 mV when v was cahnged from 15 to 200 mV s^{-1}. When v was lowered to 2 mV s^{-1} (CV not shown here), the ΔE_p for FC4VFC4 was 57 mV. For both viologens, cathodic peak current (i_{pc}) and anodic peak current (i_{pa}) at any given v were equal, and they were proportional to $v^{0.5}$. The voltammetric features were not perfectly of diffusion controlled reversible response because of the slight deviation of ΔE_p from theoretical one-electron

transfer in the absence of the influence with uncompensated solution resistance. For our present purpose, however, the use of the following equation to obtain diffusion coefficients should not represent a serious problem:

$$i_{pc} = -(2.69 \times 10^5)\, n^{3/2} A D_{ox}^{1/2} v^{1/2} C_{ox}^{*} \qquad (4\text{-}1)$$

where i_{pc} is given in the unit of A; n = 1 is the number of electron involved in the redox reaction; A is the electrode area in cm^2; D_{ox} is the diffusion coefficient of oxidized form of viologen (V^{2+}), in $cm^2\ s^{-1}$; v is given in V s^{-1}; and C_{ox}^{*} is the bulk concentration of viologen in mol cm^{-3}. The D_{ox} values for C4VC4) and FC4VFC4 were estimated to be 4.51×10^{-6} and 3.85×10^{-6} $cm^2\ s^{-1}$, respectively, based on the slopes of i_{pc}–$v^{1/2}$ plots, assuming that the electrode surface roughness was negligible.

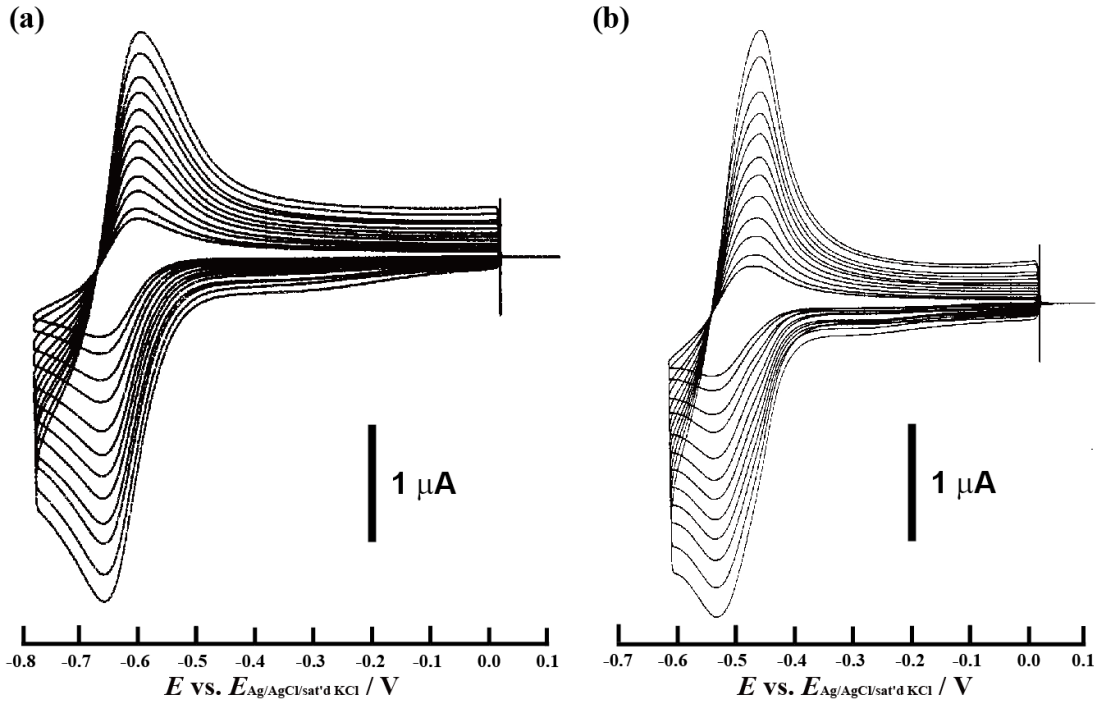

Fig. 4-1. CVs of a bare macro-Au electrode (A = 0.201cm^2) in (a) 0.5 mM C4VC4 + 0.1 M KCl solution and (b) 0.5 mM FC4VFC4 + 0.1 KCl solution. For both (a) and (b), v = 200,170, 140, 120, 100, 80, 65, 50, 35, 25, 15, 10 mV s^{-1}.

4.2.2. Voltammetric Studies at Au-UME

Steady-state voltammograms were measured at a Au-UME to evaluate the diffusion coefficients. The use of an UME has an advantage that one can ignore the contribution of adsorbed species to the current. This is because the redox current of adsorbed species, being proportional to the surface area and thus to the square of the electrode radius, i.e., r^2, is usually much smaller than the diffusional faradaic current, which is proportional to r. The redox current of adsorbed species, if there is any, decays to zero in a short period of time. The steady-state limiting current is described by Eq. (4-2) [3]:

$$i_{\text{lim}} = 4nF\, C_{\text{ox}}^{*} D_{\text{ox}} r \tag{4-2}$$

The steady-state CVs were recorded at v = 1 mV s^{-1}, and the resulting data were fitted to the Nernst equation (Eq. (3)) with n = 1.

$$i(E) = a - \frac{i_{\text{lim}}}{1 + \exp\left[\dfrac{nF(E - E^{0})}{RT}\right]} \tag{4-3}$$

The red lines in Fig. 4-2 are the fitted ones with optimal parameters a(C4VC4) = -6.58 × 10^{-12} A and a(FC4VFC4) = -2.74 × 10^{-11} A, i_{lim}(C4VC4) = -4.71 × 10^{-10} A, i_{lim}(FC4VFC4) = -2.74 × 10^{-10} A. The values of D_{ox} were then calculated from the fitted values of i_{lim} using Eq. (2).

Table 4-1 summarizes the values of E^{o}' and D_{ox} obtained for the two viologens of interest, together with those for methyl viologen (MV). The values of E^{o}' and D_{ox} obtained from two methods are consistent with one another.

Table 4-1. Formal potentials and diffusion coefficients for methyl viologen (MV), C4VC4, and FC4VFC4 obtained from the CV measurements using the macro Au electrode and Au-UME.

	Macro electrode		UME	
	$E^{\circ\prime}$ [mV]	$10^6 D_{Ox}$ [cm^2s^{-1}]	$E^{\circ\prime}$ [mV]	$10^6 D_{Ox}$ [cm^2s^{-1}]
MV	-626	7.11	-622	7.94
C4VC4	-628	4.51	-630	4.95
FC4VFC4	-498	3.85	-504	4.44

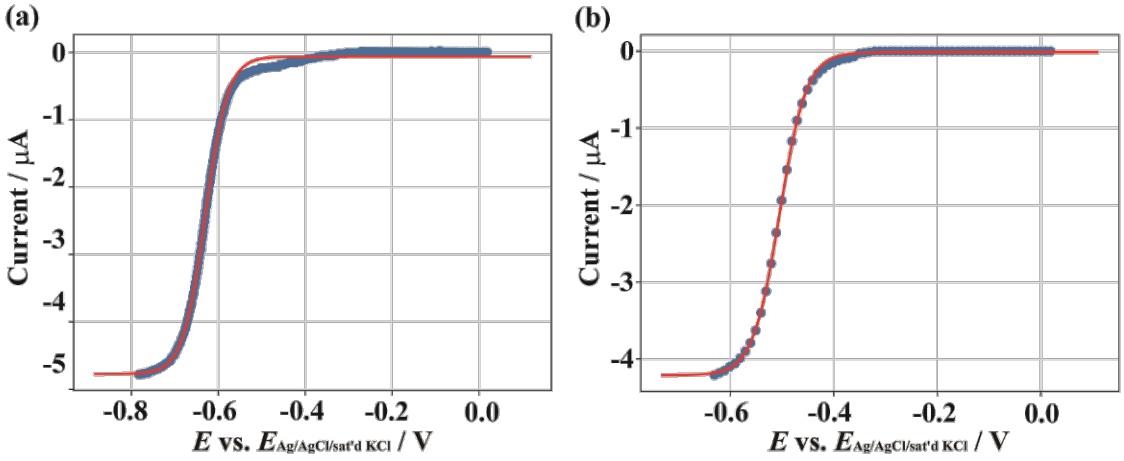

Fig. 4-2. CVs of the Au-UME (A = 74.97 μm^2) recorded at v = 1 mVs^{-1} in a 0.5 mM C4VC4 + 0.1 M KCl solution (a) and in a 0.5 mM FC4VFC4 + 0.1 M KCl solution (b). Blue circles are experimental data; whereas red curves are the best fit results.

4.2.3. DFT thermochemistry

The aqueous reduction of a viologen dication (V^{2+}) can be considered as a combination of a sequence of hypothetical reactions, as shown in Fig. 4-3. First, an aqueous V^{2+} and a solvated electron are taken from the solution to the gas phase (reaction 2, desolvation). This is followed by the combination of these two species to give the gas-phase radical monocation $V^{\bullet+}$ (reaction 3, reduction). Finally, bringing the gas-phase reduced species to water (reaction 4, solvation) completes the thermochemical cycle for the overall reaction 1. The computed values for these processes are shown in Table 2, with the contributing aqueous solvation free energy for electron (-148.5 kJ mol^{-1}) taken from literature. [4]

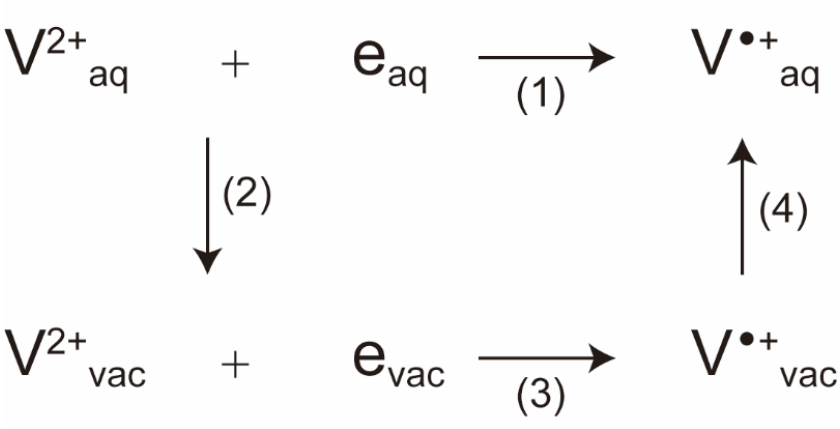

Fig. 4-3. Representation of aqueous reduction of a viologen dication (V^{2+}) using combination of a sequence of hypothetical reactions. For reactions (1) through (4), see text.

As we shall see, another interesting difference between FC4VFC4 and C4VC4 is their aqueous solubilities. Direct quantum chemistry computation of such a quantity is non-trivial. However, one can envisage that, for ionic species, the solvation of an ion pair can serve as a proxy for qualitatively comparing the solubilities of similar species. We have put this into practice by calculating the dissolution of gas-phase $(V^{n+})(Cl^-)_n$ to form V^{n+}_{aq} and $n \cdot Cl^-_{aq}$ via aqueous $(V^{n+})(Cl^-)_n$, where $n = 2$ for V^{2+} or $n = 1$ for $V^{\bullet+}$. The results are shown in Table 4-3.

Table 4-3. Computed solvation free energies (kJ mol^{-1}) of gaseous viologen chlorides [FC4VFC4 (F) and C4VC4 (H)] and their energy components

process	ΔG(F)	ΔG(H)	$\Delta\Delta G$(F - H)
$VCl_{2,vac} \rightarrow VCl_{2,aq}$	-213.2	-203.8	-9.3
$VCl_{2,aq} \rightarrow V^{2+}_{aq} + 2\ Cl^-_{aq}$	-54.1	-67.5	13.4
overall	-267.3	-271.4	4.1
$VCl_{,vac} \rightarrow VCl_{,aq}$	-131.1	-129.4	-1.7
$VCl_{,aq} \rightarrow V^{+}_{aq} + Cl^-_{aq}$	-31.5	-38.7	7.3
overall	-162.5	-168.1	5.6

4.3 Discussion

4.3.1. Formal potential Difference

The obtained $E^{o'}$ values in Table 1 show small method-to-method deviations that are less than ± 6 mV. The $E^{o'}$ value for MV is -624 $\pm$ 1 mV (Table 4-1), which compares well with the requently cited literature value of -643 mV [5,6] and thus further validates our determination. The $E^{o'}$ value of C4VC4 is in accord with the typical values of dialkyl viologen dichloride, while the value for FC4VFC4 is approximately 128 mV more positive than that for C4VC4.

The calculated difference of the Gibbs energy change, -20.6 kJ mol^{-1} (Table 4-2), which corresponds to a more positive redox potential for FC4VFC4 than that for C4VC4, is in qualitative agreement with the experimental difference. Both the desolvation step and the reduction step involve large free energy changes of approximately 800 kJ mol^{-1}. They also contribute substantially to the difference between FC4VFC4 and C4VC4. Coincidentally, the free energy difference of 49.4 kJ mol^{-1} for the desolvation step is similar in magnitude to that for the reduction step (-46.5 kJ mol^{-1}); the opposite signs of the two steps lead to a cancellation of the energy differences, such that the overall difference of -20.6 kJ mol^{-1} is similar to the difference for the final solvation processes (-23.5 kJ mol^{-1}).

Intuitively, the difference in the gas-phase reductions of FC4VFC4 and C4VC4 may be a result of two prospective effects, namely (1) direct overlap of the electron-accepting orbitals with the orbitals of the electron-withdrawing substituents through hyperconjugation, and (2) long-range electrostatic/inductive effects. The latter effect has been proposed by Hunig and Schenk to account for observations that a viologen with strong electron-drawing groups show more positive $E^{o'}$ than that with weaker electron-withdrawing groups [7]. We have briefly considered both possibilities. Regarding the effect of orbital overlap, an examination of the (viologen-based) LUMO of FC4VFC4 shows a slight extension of the orbital beyond the viologen core but it does not reach the fluorinated termini. To probe the long-range through-space effect of the C_2F_5 group, we have computed the energies for reducing analogs of FC4VFC4 that contain longer alkyl spacers (up to $–(CH_2)_5$-C_2F_5.). Extrapolation of our results shows that convergence to the value of C4VC4 is unlikely to be reached for a chain with less than ten CH_2 units.

We now turn our attention to the desolvation and solvation processes. The calculated free energies suggest a higher hydrophilicity for FC4VFC4 than that for C4VC4. Although our calculations do not provide a breakdown of contributing effects, this result can be rationalized by a greater local dipole moment of the $-C_2F_5$ group, which can be inferred from the computed Mulliken atomic charges. The difference for desolvating the dication is larger than that for solvating the monocation, as one would intuitively expect.

Overall, two of the three component processes in the thermochemical cycle of Fig. 4-3 favor the reduction of FC4VFC4 over that of C4VC4; the strong through-space electron-withdrawing nature of C_2F_5 leads to a more facile intrinsic (gas-phase) reduction for FC4VFC4, and the more polar FC4VFC4 radical monocation solvates better than the less polar C4VC4. These effects overcome the larger energy penalty for desolvating FC4VFC4 dication relative to desolvating C4VC4 dication, as a whole yielding a more favorable aqueous reduction of FC4VFV4.

4.3.2. Diffusion coefficients

The two methods of measurements both gave smaller D_{ox} for FC4VFC4 than those for C4VC4 by 10-15 %. Estimation of D_{ox} can be made using the Nernst-Einstein equation:

$$D_{ox} = k_B T/6\pi\eta r_s \qquad (4\text{-}4)$$

where k_B is the Boltzmann constant, η is the viscosity, r_s is the Stokes radius of the particle as approximated by a sphere. Our DFT calculations in the preceding section also provide us with the information regarding the structure of the viologens; for both oxidation states and for both compounds, conformations with extended side chains are more stable than the, inward-point, bent side chain conformations. This implies that there should be little difference in r_s between the two compounds, and the cause of the difference of D_{ox} is by other factors. A potential cause of the smaller diffusion coefficient of perfluoalkyl viologen is difference in the structures of water clusters surrounding and the highly polar perfluoalkyl $-C_2F_5$ moiety. This possibility will be investigated in future studies.

4.3.3. Aqueous solubility

The oxidized form of FC4VFC4 is water-soluble, although its saturated concentration was found to be lower than 1 mM. In contrast, C4VC4 has a much higher solubility than FC4VFC4 does. This observation seemingly contradicts the higher hydrophobicity of FC4VFC4 than the hydrophobicity of C4VC4, as discussed in the previous session on the basis of the results of Table 4-2. However, the discussion of solubility should also take the interaction with the counterion into account. Separately, to investigate the effect of the chain length on the solubility, we synthesized 1*H*,1*H*,2*H*,2*H*-perfluorohexyl-4,4'-bipyridinium iodide, and found it to be completely insolubile in water, even though the hydrocarbon analog diheptyl viologen is soluble.

Our DFT Gibbs free energy changes for the process of solvating and ionizing gas-phase $(V^{2+})(Cl^-)_2$ and $(V^{\bullet+})(Cl^-)$ to give, respectively, $[V^{2+}_{aq} + 2Cl^-_{aq}]$ and $[V^{\bullet+}_{aq} + 2Cl^-_{aq}]$ (Table 4-3) are consistent with experimental observation that FC4VFC4 is less soluble than C4VC4. The energies for component elementary steps of the overall dissolution indicate that the fluorinated species are more soluble as ion pairs in comparison with the corresponding ion pairs of the hydrocarbon. However, the stronger binding with the counter ions for FC4VFC4 dominates, which hinders the ionization step and as a result leads to an overall lower solubility than the non-fluorinated viologen species.

4.4 Conclusions

We present a detailed investigation of the solution electrochemistry of the perfluorinated viologen (FC4VFC4), which reveals the effect of sidechain fluorination on the physicochemical properties. The oxidized form of FC4VFC4 has a more positive formal potential and a lower diffusion coefficient in water than C4VC4. The positive shift of formal potential E^{o}' arose from strong electron-withdrawing effect of the perfluorinated groups, despite a separation of $(CH_2)_2$ from the viologen core. Two probable contributing factors to the positive shift are considered: (1) contribution of C_2F_5 unit to the electron-accepting LUMO, and (2) long-range electrostatic/inductive effects of the C_2F_5 unit. Our DFT computations indicate that the latter effect is substantial, with a C_2F_5 unit showing

considerable effects on $E^{o'}$ for substrates with up to approximately ten CH_2 units of separation.

The lower D_{ox} of FC4VFC4 when compared with C4VC4 is not likely to be a result of conformational differences of the two molecules in water. We find that the fluorinated compounds to be generally less soluble in water than their hydrocarbon counterparts. Our calculations suggest that fluorination facilitate solvation of bare ion pair of the viologen and its counter ions. The stronger binding with thse counter ions, however, gives rise to a lower solubility than the non-fluorinated viologen species. This is consistent with the report of Hasegawa and coworkers. [8]

Finally, this perfluoro viologen is water-soluble in both oxidation states and is expected to be used as a redox probe at electrified oil-water and fluorous phase-water interfaces.

References (Chap. 4)

[1] A. Moiodek, H. Q. A. Lê, H. S.-Dorizon, H. K.-Youssoufi, Streptavidin-polypyrrole Film as Platform for Biotinylated Redox Probe Immobilization for Electrochemical Immunosensor Application, Electroanalysis 28 (8) (2016) 1824-1832.

[2] R. P. Singh, J. M. Shreeve, Syntheses of the first N-mono- and N,N'-dipolyfluoroalkyl-4,4-bipyridinium compounds, Chem. Commun., (2003) 1366-1367.

[3] Y. Saito, A Theoretical Study on the Diffusion Current at the Stationary Electrodes of Circular and Narrow Band Types, Rev. Polarogr. 15 (6) (1968) 177-187.

[4] C.-G. Zhan, D. A. Dixon, The Nature and Absolute Hydration Free Energy of the Solvated Electron in Water, J. Phys. Chem. B 18 (107) (2003) 4403-4417.

[5] L. Michaelis, E. S. Hill, J. Gen. Physiol. 16 (6) (1933) 859-873.

[6] L. Striepe, T. Baumgartner, Viologens and Their Application as FunctionalMaterials, Chem. Eur. J. 67 (23) (2017) 16924-16940

[7] S. Hunig, W. Schenk, Liebigs Ann. Chem. 10 (1979) 1523-1533.

[8] T. Hasegawa, Physicochemical Nature of Perfluoroalkyl Compounds Induced by Fluorine, Chem. Rec. 17 (10) (2017) 903-917.

Chapter 5

Electrochemical and spectroelectrochemical probing of the ionic channel in Nafion films using the redox of perfluoroalkyl viologen

ABSTRACT. We explored the electrochemistry of a perfluoroalkyl viologen, *N*,*N*'-di-(1*H*,1*H*,2*H*,2*H*-perfluorobutyl)-4,4'-bipyridinium dichloride (FC4VFC4) in a Nafion film on an Au electrode. The capability of FC4VFC4 as a redox-active probe for micro-environments of the ionic channels in the Nafion film was highlighted by clarifying the difference of its electrochemical behavior from that of its alkyl analog, dibutyl viologen (C4VC4). The time course of cyclic voltammograms (CVs) was tracked after immersion of a Nafion film-coated Au electrode in viologen solutions of various concentrations, C_s. The strongly C_s-dependent time change revealed the formation of an aggregate of FC4VFC4 in the ionic channels in the Nafion film. The aggregate blocks its own redox reaction at $C_s \geq 10$ μM. At $C_s = 5$ μM, FC4VFC4 exhibited a quasi-reversible response. In contrast, C4VC4 showed a quasi-reversible response in the C_s range from 5 μM to 200 μM. We also used the time dependent change of electroreflectance (ER) spectra to track the state of viologens in the close proximity of the electrode|Nafion interface. After the immersion in 50 μM FC4VFC4 solution, the ER signals of the redox of FC4VFC4 molecules, being not in direct contact with the Au surface, rapidly increased in line with the change of CVs. What followed was a steep decrease of ER signal while the CV redox current was still increasing. It was also found that the FC4VFC4 aggregates in the Nafion film block the electrode reactions of $[Ru(NH_3)_6]^{2+/3+}$, methylviologen, and C4VC4, which otherwise show reversible or quasi-reversible responses in the absence of FC4VFC4. All the results, especially the sharp contrast of the behavior of FC4VFC4 to that of C4VC4, revealed that either or both intermolecular perfluoro chain-chain interaction and perfuorinated FC4VFC4 side chain-Nafion perfluoroether side chain interaction are the key to determine the chemical micro-environment in the ionic channels.

5.1. Introduction

A Nafion film immersed in water has a phase-separated structure composed of a micro water-phase and a perfluoroalkyl-phase. Because of the characteristic micro water-phase network structures, chemical micro-environment in a Nafion film has a specific electrostatic and hydrated nature. Studies on the basis of the two-phase framework model with the water-phase and perfluoroalkyl-phase were extensively conducted through various approaches from a viewpoint of micro-structures of hydrated Nafion films. Using the results of spectroscopic measurements of hydrated Nafion films by X-ray reflection and scattering and neutron-ray diffraction, a variety of nanoscopic and mesoscopic structure models have been proposed [1-7]. Inaba and co-workers pointed out the importance to consider the third phase enriched by the perfluoroether sites at the boundary of the aforementioned two phases [8]. Whichever two- or three-phase model is used, an understanding of chemical micro-environment of a Nafion film would provide us with an indispensable and practical guide to newly design a proton transporting membrane, because Nafion presently represents one of the best materials for polymer electrolyte fuel cells. We may also expect new applications of Nafion as a bi-continuous phase-separated material.

The viologens exhibited superior molecular probe features, because they have reversible electrochemical activity. Both oxidized (V^{2+}) and one-electron reduced ($V^{\bullet+}$) forms are cationic species possessing affinity to the anionic sulfonate groups in the ionic channel of Nafion. Strongly colored nature of $V^{\bullet+}$-forms enables us to follow the state of viologen by visible spectroscopies. To our best knowledge, however, redox probes have been restricted so far to cationic and hydrophilic ones, which are perfluoro-repulsive. This has limited the obtainable properties of the micro-environments in Nafion. To shed light in more depth of the ionic channels, the use of a probe having a perfluoroalkyl affinity should be meaningful.

In this work, we use a perfluoroalkyl viologen redox probe, *N*,*N*'-di-(1*H*,1*H*,2*H*,2*H*-perfluorobutyl)-4,4'-bipyridinium dichloride (FC4VFC4), bearing perfluoroalkyl side chains. Electrochemical properties of FC4VFC4 have been reported elsewhere [9]. In the light of the above-mentioned diameter of the channel, the molecular size and water-solubility should allow for penetration of FC4VFC4 into Nafion films. FC4VFC4 in the Nafion film may have affinities to both perfluoroalkyl-phase and sulfonate groups simultaneously. We use a

Nafion-coated polycrystalline Au electrode in the aqueous solution of FC4VFC4 and dibutyl viologen (C4VC4). C4VC4 is the alkyl analog of FC4VFC4 as a reference substance to highlight the effect of perfluorination of the side chains. Scheme 1(in Chapter3) shows molecular structures of the two viologens. In addition to voltammetric measurements, electroreflectance (ER) spectral measurements are made to focus on the states and electron transfer reactions of viologen in a close proximity of the Au electrode surface. We also track the penetration of viologen into the Nafion film by a combined use of CV and ER data.

5.2. Results and Discussion

5.2.1. Voltammograms at a Nafion coated Au electrode.

The Nafion-coated Au electrode showed pronounced changes of CV with time. At given C_s, CVs at 200 mV s^{-1} were intermittently measured until reaching saturation. The total number of potential scans was restricted to prevent the CV from being influenced by the scans themselves. We monitored the redox reaction of $V^{\bullet+}/V^{2+}$ couple, $V^{2+} + e^-$ (electrode) $\rightleftharpoons$ $V^{\bullet+}$, and we did not scan the potential region of further reduction of $V^{\bullet+}$.

5.2.1.1 C4VC4 at 500 μM

Fig. 5-1 shows the results of CV measurements in a 500 μM C4VC4 + 0.1 M KCl solution at a Nafion-coated Au electrode. Immediately after the immersion, a viologen redox peak pair appeared at E_m = -0.690 V (black line of t = 0 min in Fig. 1-a) together with a cathodic peak of residual oxygen reduction around -0.42 V. It is known that a bare Au electrode in 500 μM C4VC4 solution shows an electrochemically reversible CV response at E_m = -0.628 V [10]. A close look at the line of t = 0 min in Fig. 1-a ensures the absence of any trace of additional cathodic current ascribable to the reduction reaction of viologen between -0.63 V and -0.68 V; this is the proof for the Nafion-coated electrode prepared in this work that any macroscopic bare Au electrode area was not exposed to the solution. At t = 30 min, both the anodic peak current i_{pa} and the cathodic peak current i_{pc} reached maxima and then decreased slowly to be steady state values at t > 700 min. In a separate experiment, we stopped the time-course tracking at certain t and recorded sweep rate (v) dependence of CV (not shown here). The

peak currents were proportional to the square root of v in the range of 10-200 mV s^{-1} regardless of t, indicating that diffusion of viologen largely determines the CV response.

Provided that the diffusion coefficient of the reduced form, D_{Red}, in Nafion is close to that of the oxidized form D_{Ox}, E_m can be approximated to the formal potential; it shifted from -0.690 V to less-negative to -0.595 V at 60 min, then shifted to slightly negative to reach a steady-state value, -0.620 V. The peak separation $\Delta E_p = E_{pa} - E_{pc}$ increased from 114 mV at 5 min to 372 mV at 360 min. The peak separations were larger than the ideal value for electrochemically reversible response of solution species (57 mV), indicating the sluggish electron transfer process at the electrode surface, the significant film resistance R_u, or non-negligible effect of migration because of the relatively low concentration of electrolyte cation. The quantitative analysis of the migration effect will be dealt with in our future work.

To examine the effect of R_u on CV, we measured electrolyte KCl concentration (C_{KCl}) dependence for 500 μM methyl viologen (MV) solution. The value of ΔE_p of the CV response of $MV^{\bullet+/2+}$ became greater with decreasing C_{KCl}; ΔE_p = 65 mV for C_{KCl} = 1.0 M, 101 mV for 0.1 M, and 226 mV for 0.01 M. The peak current at C_{KCl} = 1.0 M is about 1/5 of that with C_{KCl} = 0.1 M, indicating that partitions of MV^{2+} and K^+ from the solution phase into the Nafion film are competitive against each other. The higher C_{KCl} gives a lower MV concentration in the film and a higher ionic conductance through the ionic channel networks in the Nafion film, resulting in the decreases in both R_u and ΔE_p. The decrease of C_{KCl} elevated R_u and increased the saturated concentration of MV in the Nafion film. On the basis of the aforementioned results, the increase of ΔE_p with time can be attributed to the decrease of the electrolyte concentration in the Nafion film by the penetration of C4VC4. It is known that the ionic channel diameter depends on ionic composition in the channel [10]. Possibility of additional effect of narrowing of the ionic channel cross-section with time on the increase of ΔE_p is expected. In Fig. 5-1, we observed a rapid positive shift of E_m in the first 30 min. This would correspond to the increased fraction of $V^{\bullet+}$-dimers over its monomers in the reduction products. It is known that the formal potential of the dimer is more positive than that of a monomer [11].

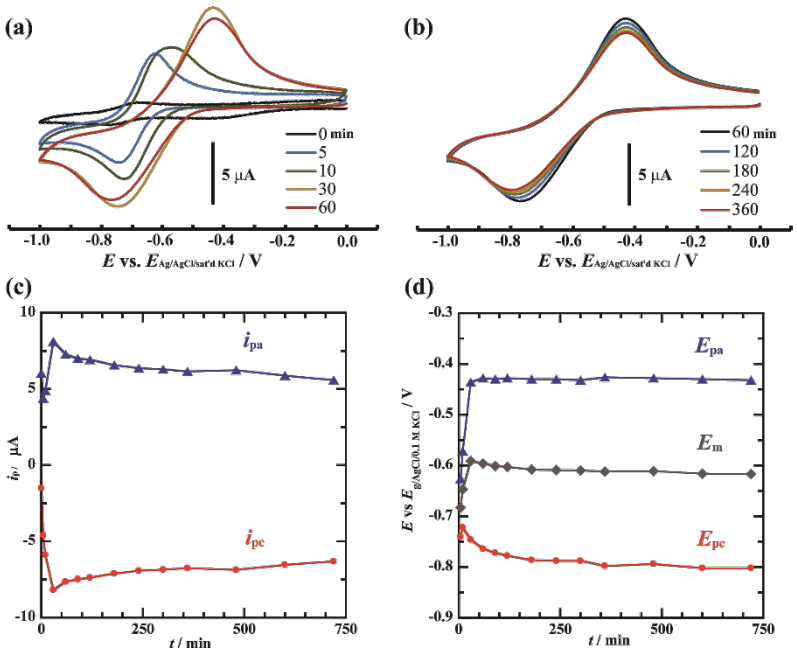

Fig. 5-1. Time-course CVs for a Nafion-coated Au electrode (A = 0.201 cm^2) recorded in a 500 μM C4VC4 + 0.1 M KCl solution at v = 200 mV s^{-1} (a and subsequently b), and plots of peak currents (c) and peak potentials (d) *versus* time.

5.2.1.2. FC4VFC4 at 500 μM

Fig. 5-2 shows the results of the time course CV measurements in a 500 μM FC4VFC4 + 0.1 M KCl solution. The increase of the peak current in the first 10 min was followed by a steep decrease. After 30 min, the cathodic peak ranged out of the negative end of the potential scan, *viz.* E_{pc} < -0.8 V. Finally, the CV reached a steady-state irreversible waveform after 720 min (Fig. 5-2-b). Fig. 5-2-c shows the time-dependent peak currents, and Fig. 2-d does the time-dependent peak potentials. Until 10 min after immersion, CVs exhibit distinct cathodic and anodic peaks, giving E_m around -585 mV. After the cathodic peak went out of the negative potential scan range, the anodic peak was still observable but gradually became smaller. FC4VFC4 displayed quite different behavior from C4VC4 at the same C_s (500 μM). The irreversible response of FC4VFC4 indicates its very sluggish electron transfer at the Au electrode surface and/or a very large R_u.

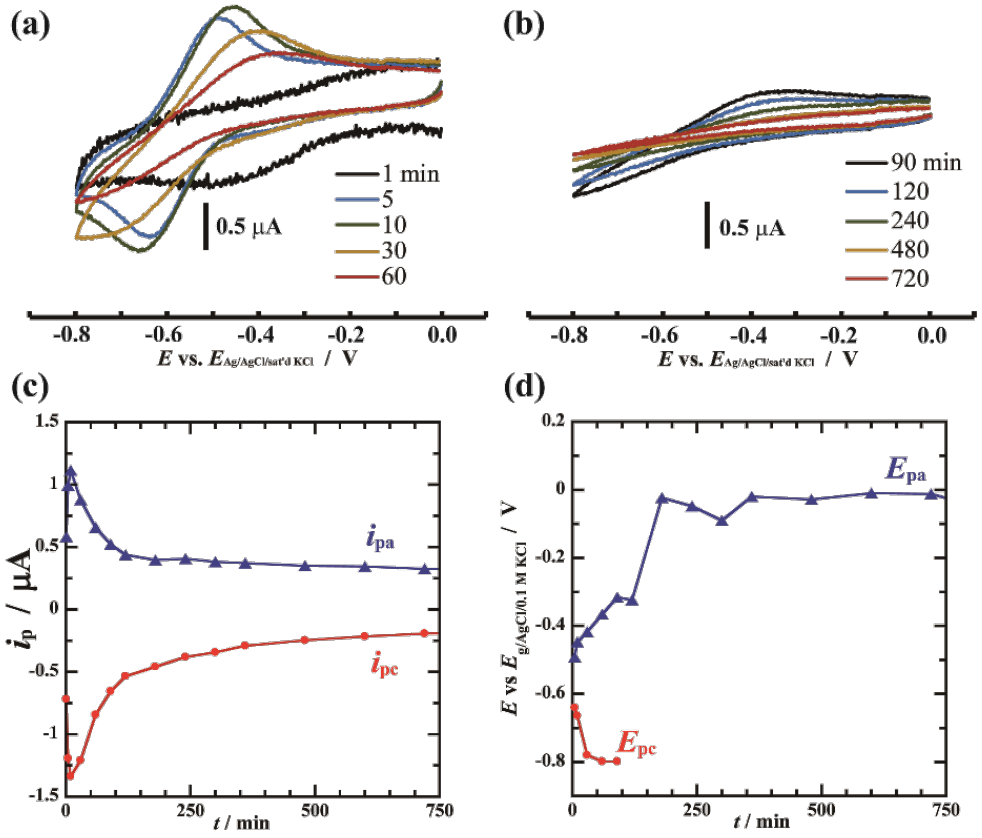

Fig. 5-2. Time-course CVs for a Nafion-coated Au electrode (A = 0.201 cm^2) recorded in 500 μM mM FC4VFC4 + 0.1 M KCl solution at v = 200 mV s^{-1} (a and subsequently b), and plots of peak currents (c) and peak potentials (d) *versus* time. The peak was distinctly observed until at the measurement of 240 min.

5.2.1.3. C4VC4-concentration dependence

Fig. 5-3-a shows the steady-state CVs for a Nafion-coated Au electrodes in C4VC4 solutions of three different C_s. The ΔE_p increased with the increase of C_s (184 mV at 5 μM, 254 mV at 50 μM, and 386 mV at 500 μM). Fig. 5-3-b shows the time dependence of i_{pc} after immersion in C4VC4 solutions. The absolute values of i_{pc} remained in the range of 4 - 8 μA, even though C_s differed by two orders of magnitude. This fact does not necessarily indicate that the amount of incorporated C4VC4 in the Nafion interior at C_s = 5 μM has already reached upper limit of the incorporation. The peak current should depend on several factors such as the surface concentration of V^{2+} in the proximity of the electrode surface, the

diffusion coefficient, the active electrode area (the total surface area with which the water phase in ionic channels are in contact), the electron transfer rate constant k_s, and R_u. Although the surface concentration of viologen increases with time in the Nafion film, if the diffusion coefficient decreases and R_u increases because of the environmental change with the increased amount of viologen, the redox current cannot increase.

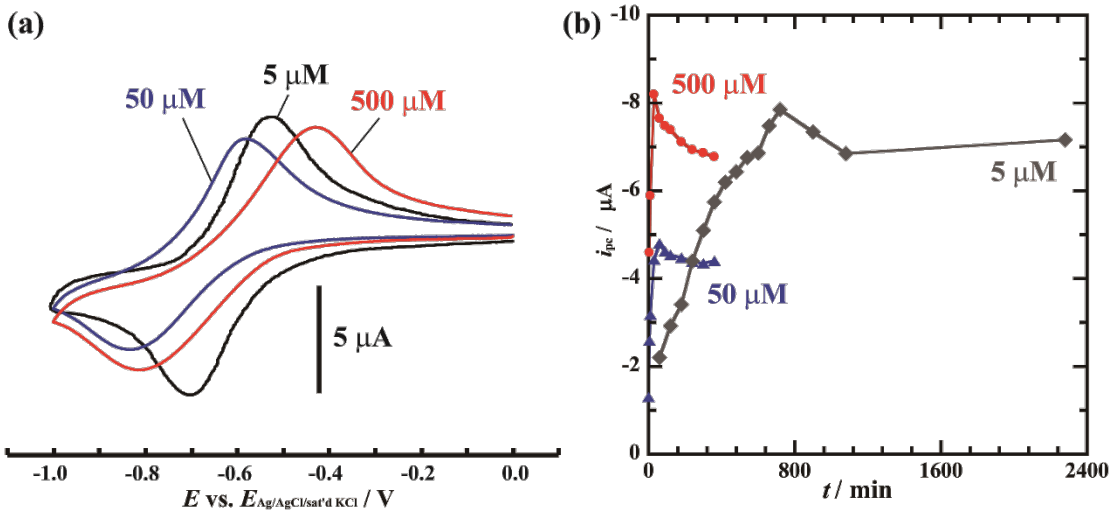

Fig. 5-3. Comparison of the steady-state CVs of a Nafion-coated Au electrode (A = 0.201 cm^2) at three concentrations of C4VC4 with the base electrolyte of 0.1 M KCl at v = 200 mV s^{-1} (a), and the time dependence of cathodic peak currents (b).

5.2.1.4. FC4VFC4-concentration dependence

Fig. 5-4-a shows steady-state CVs reached in the time-course measurements with three different C_s of FC4VFC4. Fig. 5-4-b shows the time dependence of i_{pc}. Intriguingly, a better-defined redox response in CV was observed at a low concentration FC4VFC4 (5 μM) rather than at higher C_s. This concentration dependence is largely different from that of C4VC4 (Fig. 5-3). At 500 μM and 50 μM, a short time increase of i_{pc} was followed by sudden turndown to decrease (Fig. 5-4-b), resulting eventually in a significantly irreversible response. A similar trend was observed at 20 μM and 10 μM. The time period before the turndown is longer at lower C_s. To reach irreversible response after the current decrease, it took 1250 min at 20 μM and 4500 min at 10 μM. However, the redox current measured at 5 μM

monotonically increased to reach a steady-state value, which was constant for over a few days at least. The CV at the steady-state was quasi-reversible, showing both cathodic and anodic redox current peaks with ΔE_p = 323 mV. We can conclude that there is a threshold concentration in between 5 and 10 μM to determine whether the critical damping of the CV of FC4VFC4 occurs or not.

To make the situation clear, it is desirable to estimate the concentration of FC4VFC4 in the film when C_s = 5 μM. It is known that, if a slow v limit of CV gives a thin-layer electrochemistry, the integrated charge of the CV peak should correspond directly the amount of active species [12]. Such a situation is realized when the partition at the film/solution interface is slow enough or diffusion in the film is much slower than the diffusion in the solution phase. Therefore, we measure the v-dependence of CV. The peak current was proportional to $v^{1/2}$ down to 1 mV/s, and the CV was still of reversible diffusion limited type with the peak-to-peak separation being 70 mV. The further decrease in v down to 0.1 mV/s altered the CV to a sigmoidal waveform attributable to the EC type reaction (electrocatalytic reaction) of residual oxygen plus apparent diffusion process of the viologen. Unfortunately, the present Nafion film/viologen systems for both C4VC4 and FC4VFC4 do not adopt to this classical method of estimation.

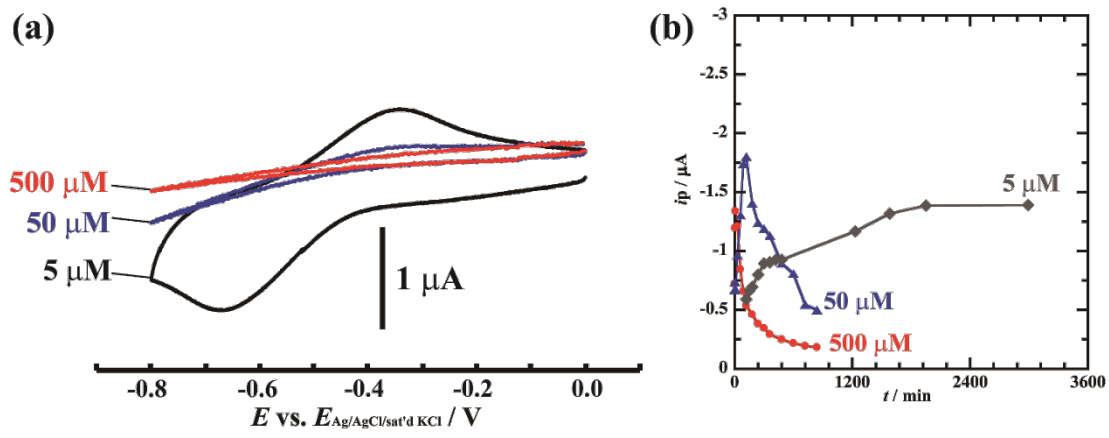

Fig. 5-4. Comparison of the steady-state CVs a Nafion-coated Au electrode (A = 0.201 cm^2) recorded at three concentrations of FC4VFC4 with the base electrolyte of 0.1 M KCl at v = 200 mV s^{-1} (a), and the time dependence of the values of their comparison of cathodic peak currents (b).

5.2.2. ER studies at Nafion coated Au electrode

The conventional voltammetric techniques alone cannot shed direct and real-time light on the state of the viologen molecules reacting near the electrode surface. Among various *in situ* spectroscopic methods, UV-visible light reflection has advantages over others, because a viologen-incorporated Nafion film is transparent in the colorless oxidized state, and one-electron reduced viologen has strong absorption bands in the UV-Vis-near IR region. In the measured λ range in this work, V^{2+}-form is colorless, whereas $V^{\bullet+}$-monomer form has absorption bands at ca. 400 nm and 602-604 nm, and $V^{\bullet+}$-dimer form does at ca. 367 nm, 536 nm, and ca. 850 nm. The isosbestic point of monomer and dimer is at 552 nm. We can also distinguish $V^{\bullet+}$-monomer and dimer from the spectrum. The phase retardation of the ac reflectance signal from E_{ac} enables us to estimate k_s. Semi-quantitatively, the intensity ratio of real and imaginary part signals at a given λ, which is abbreviated as "r/i-ratio", is an indicator of the heterogeneous electron transfer rate; the greater the ratio, the greater the value of k_s [13]. Applying an ac potential modulation E_{ac}, we can selectively observe the viologen molecules undergoing the redox interconversion that gives the ac spectroscopic signal at the same frequency as E_{ac}. The phase retardation may originate from the slow electron transfer kinetics as well as the nonzero cell time constant determined by the double-layer capacitance, the film resistance, and bulk solution resistance. The r/i-ratio enables us to discuss the kinetics. Taken together, the ER method, namely potential-modulated UV-vis reflectance spectroscopic method, provides us with highly valuable information of the interfacial reaction of viologen molecules. Unless the redox reaction involves the surface-deposited dense phase of colored electroactive species, an ER spectrum representing the redox reaction shows a difference absorption spectrum: the absorption spectrum of reduced form from which that of the oxidized form is subtracted [13,14].

In Fig. 5-5, the initial ER spectrum at 4 min in C4VC4 solution shows no redox response of viologen but a weak and broad ER signal from the Au surface as a negative-going real part response with a maximum around 500 nm [13] (also seen in Fig. 5-6-a). Growths of the ER signals of the redox reaction of viologens were obvious from 18 min in C4VC4 solution and from 19 min in FC4VFC4 solution. Because $V^{\bullet+}$-forms have strong visible absorptions but V^{2+}-form is colorless, the redox ER signals showed positive-going real parts and negative

going imaginary parts. Because no surface deposition of $V^{\bullet+}$-forms took place, the spectral structure of the obtained redox ER signal was of the difference absorption spectral type.

In C4VC4 solution, the response of $V^{\bullet+}$-monomer at ~603 nm was first built up exclusively, and a rapid growth of the dimer signal at ~537 nm followed. The dimer signal became predominant over the monomer one after ca. 190 min. The same trend occurred in FC4VFC4 solution from much earlier time (30 min) than that in C4VC4 solution. These results confirmed that the ionic channel provides a volume for both C4VC4 and FC4VFC4 enough to find partner to form dimers. In addition, the concentration of $V^{\bullet+}$ became high enough to form its dimers by successive ingress of the viologens from the solution phase. In sharp contrast to the monotonical ER signal growth in C4VC4 solution for 500 min, the ER signal in FC4VFC4 solution decreased drastically after 163 min. After 4 h, the ER signal of FC4VFC4 redox almost disappeared.

Fig. 5-6 shows typical ER spectra taken from Fig. 5-5. The zero-line is now added. Because the ER signal from the Au surface (Fig. 5-6-a) is relatively weak, provided that the cell time constant never affects the phase of redox ER signal, we can now discuss the r/i-ratio. In Fig. 5-6, with an increase in the ER signal of C4VC4, the r/i-ratio became smaller at both 537 nm and 603 nm. In contrast, ER spectra in FC4VFC4 solution exhibited a different r/i-ratio at 603 nm from that at 537 nm; for example, at t = 123 min the former was greater than the latter (Fig. 5-6-e). The ratio was also a function of t. We can learn from Figs. 5-5 and 5-6: (i) The redox process of the monomer became sluggish with time for both C4VC4 and FC4VFC4, and (ii) The redox reaction of $V^{\bullet+}$-dimer/V^{2+} couple is relatively slower than that of $V^{\bullet+}$-monomer/V^{2+} couple. The following section is devoted to the discussion about the time-dependent features by combined use of CV and ER data.

5.2.2.1. Time-dependent behavior observed by CV and ER.

It is crucial to perceive the diffusion layer thickness of viologen in the Nafion film when measuring CV. Using a rotating-disk electrode (RDE) technique as follows, we confirmed that the diffusion layer thickness is thinner than the thickness of the hydrated Nafion film as far as $v > 1$ mV s^{-1} is used. First, RDE measurements in 0.5 mM MV solution were made for a hydrated Nafion film-coated Au-RDE. The film thickness was set as the same as that on the stationary Au electrode. We found that the CVs at $v > 1$ mV s^{-1} were never affected by the

on-off of the rotation. In contrast at $v < 1$ mV s^{-1}, CV became smaller when stopping the rotation. The change of CV occurred when the tail end of the diffusion layer reached to the Nafion|solution interface. Second, recall that in the aqueous solution phase, the diffusion coefficients of C4VC4 and FC4VFC4 are 63.4% and 54.1% of that of MV in aqueous solution [23]. This fact gives a rationale behind the assumption that the diffusion coefficients of C4VC4 and FC4VFC4 in Nafion are also smaller than MV. Taken together, as far as a sweep rate of 200 mV s^{-1} is used, the tail of the diffusion layer is well inside of the Nafion film.

We should note the difference between a wide potential range CV and a smaller amplitude potential-modulated ER to gain comprehensive understanding of the spatiotemporal behavior. In CV measurements, the potential was scanned almost over the range of cathodic and anodic peaks, namely 0.0 to -1.0 V. When the CV current takes its peak, the diffusion layer is largely extended from the electrode surface to the interior of the Nafion film. On the other hands, in ER measurements, the electrode potential was repeatedly changed around E_{dc}, set at the formal potential, with a peak-to-peak amplitude of 113 mV. The concentration profiles of the diffusion layer are of undulated waves decaying from the electrode surface to the direction of the film interior. The thickness of the undulated concentration profile is much smaller in ER measurements than the extended diffusion layer in the CV measurements. The ER method can detect the change of the concentration ratio $V^{\bullet+}/V^{2+}$ at the close proximity of the Au surface. By the use of ER signals, the electron transfer kinetics is roughly represented by the r/i ratio. The magnitude of the redox ER signal is represented by

$$I_{ER} = [(\Delta R/R)_{real}^2 + (\Delta R/R)_{imag}^2]^{1/2} \quad (2)$$

where I_{ER} reflects the amount of viologens interconverted between oxidized and reduced states in response to E_{ac}; I_{ER} is greater when more viologens are reacted with faster kinetics [24].

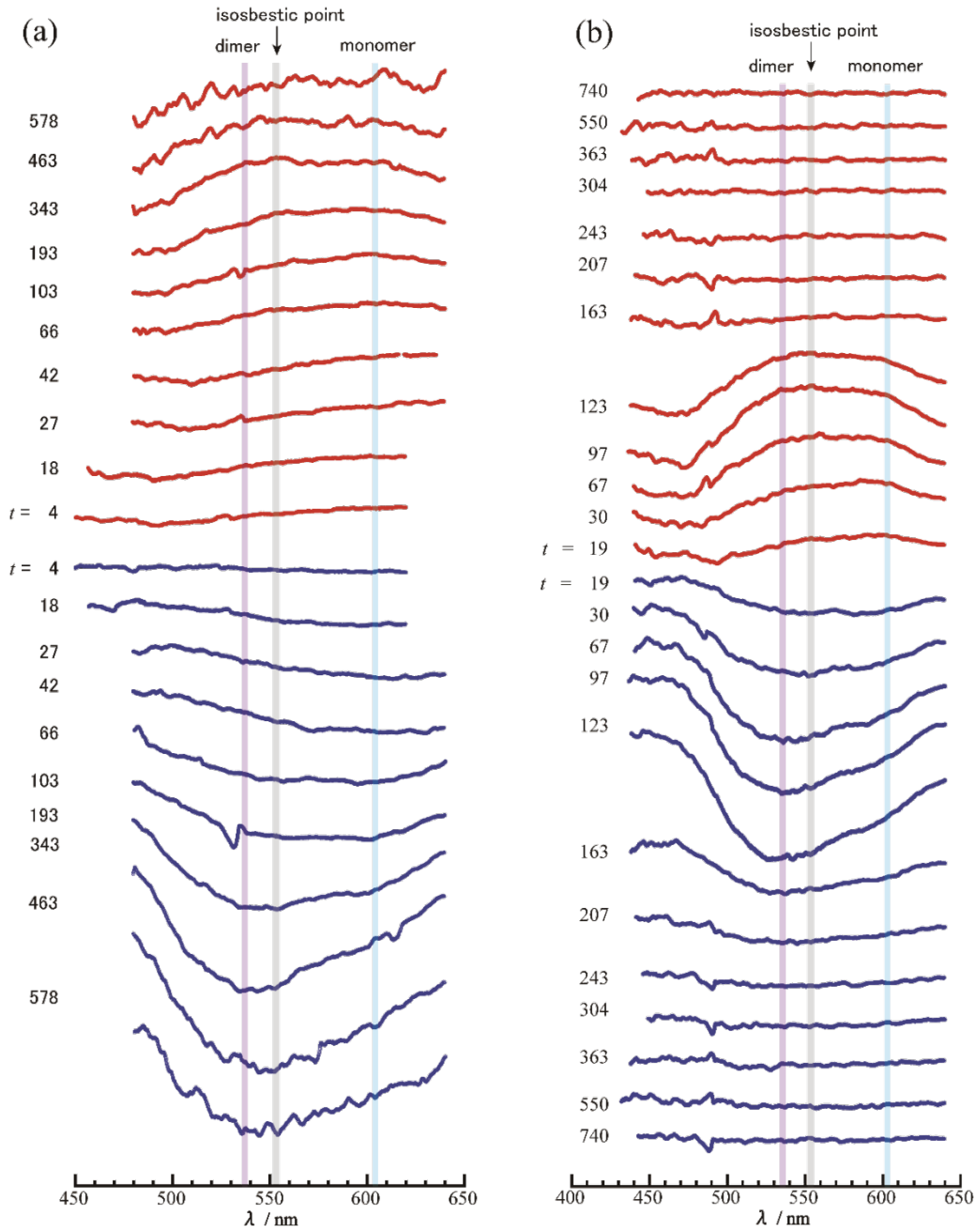

Fig. 5-5. Change of ER spectra with time after immersion of a Nafion-coated Au electrode in 50 μM C4VC4 + 0.1 M KCl solution (a) or 50 μM FC4VFC4 + 0.1 M KCl solution (b). E_{dc} for the potential modulation (see Eq. [1]) was set at the E_m in the latest CV before the wavelength scan. Positive-going spectra (upper-going curves with red color) are of the real part, whereas negative-going spectra (lower-going curves with blue color) are of the imaginary part.

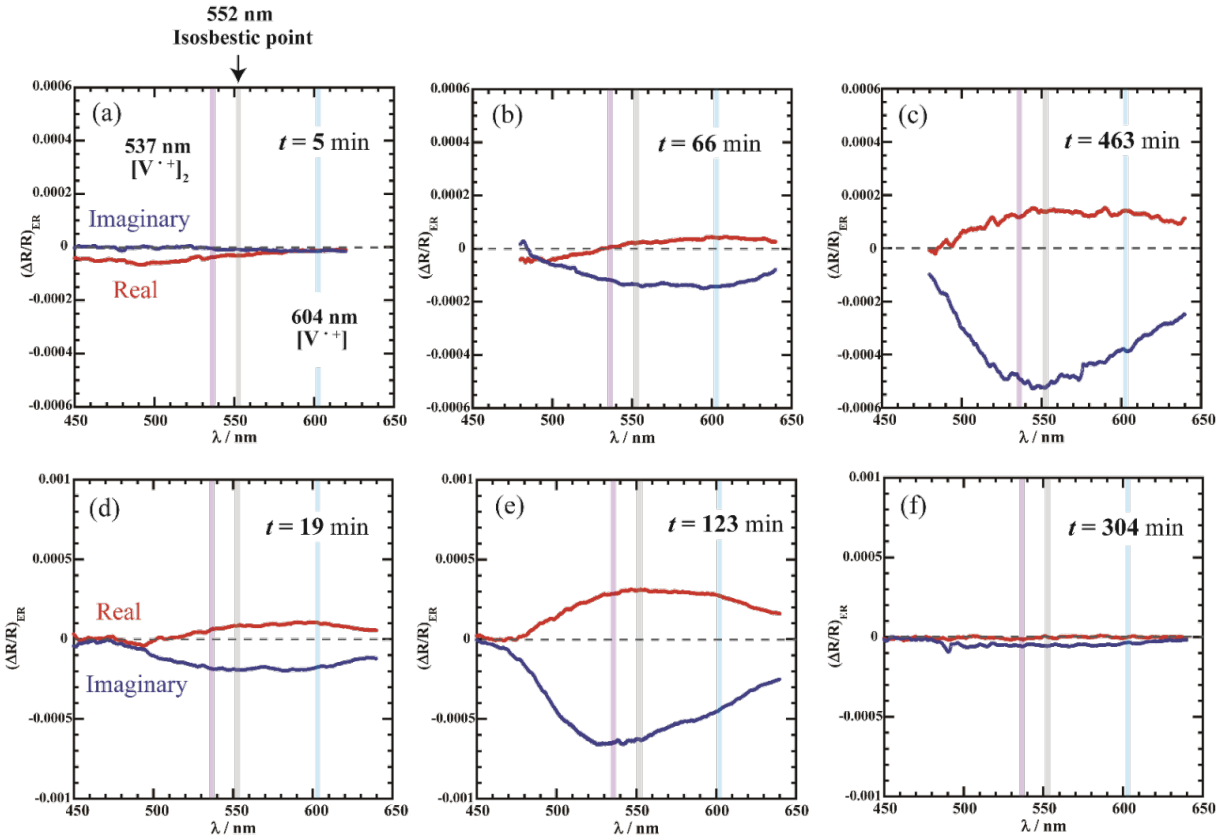

Fig. 5-6. Selected ER spectra obtained in 50 μM C4VC4 + 0.1 M KCl solution (a-c) and in 50 μM FC4VFC4 + 0.1 M KCl solution (d-f).

In Fig. 5-7, we can find the correlation among the CV cathodic peak current i_{pc}, CV peak separation ΔE_p, ER signal magnitude I_{ER}, and the r/i ratios. As far as the region of $t < 350$ min is concerned in 50 μM C4VC4 + 0.1 M KCl solution, the time dependence of I_{ER} was in line with i_{pc}. The increase of I_{ER} at 537 nm was steeper than that at 602 nm, indicating a steeper increase of the amount of $V^{\bullet+}$-dimer than the increase of $V^{\bullet+}$-monomer. In the region of $t >$ 300 min, ΔE_p was almost constant, indicating that the electron transfer kinetics was unchanged and that iR drop caused by R_u was not substantial.

Taking a look at the time region of $t < 300$ min in 50 μM FC4VFC4 + 0.1 M KCl solution, we find sharply different time course behavior from that of C4VC4:

(i) Initially, the increases of I_{ER} and i_{pc} took place in parallel with keeping ΔE_p constant.

(ii) ΔE_p steeply increased after 163 min.

(iii) Before the increase of ΔE_p started, I_{ER} started decreasing at 97 min, while i_{pc} was still increasing

(iv) i_{pc} turned to decrease after I_{ER} reached to less than 30% of its maximum.

(v) When ΔE_p exceeded 400 mV, I_{ER} reached to less than 10% of its maximum.

(vi) When the ER signal further decreased to be almost zero, the cathodic peak went out of the scanned potential range.

The decrease in I_{ER} and the following increase in ΔE_p indicate that the interfacial electron transfer kinetics became sluggish or an increase in R_u occurred. We did not see any signature of the surface deposition of FC4VFC4 in the ER spectra. The r/i ratios of FC4VFC4 indicated that the monomer redox process is always faster than dimer reaction (Fig. 5-7-f), and for C4VC4 as well (Fig. 5-7-c).

If the decay of the redox response of FC4VFC4 is due to only the electron transfer kinetics, the increase of ΔE_p and the decreases of i_{pc} and r/i ratios should have occurred with the same time dependency. Because the observation is not in line, the time dependence originated from not only the slower kinetic but also slower diffusion and greater R_u but asynchronously. Therefore, a sudden change of the electron transfer kinetics alone is not likely.

Fig. 5-8 shows dimer/monomer ratios calculated from Figs. 5-7-b and e applying Gao's method [15]. The values of I_{ER} at absorption maxima of monomer at 603 nm and dimer at 537 nm were used to calculate the ratio. The dimer/monomer ratio of C4VC4 was as low as 0.05 at the initial stage. Then, it increased to reach a constant value around 0.4 at 343 min, indicating that the concentration of the $V^{\bullet+}$-form of C4VC4 near the Au electrode surface attained saturation. In Fig. 5-1-d, it took much shorter time, 30 min, to reach saturation of the dimer content ratio in the solution of 500 μM C4VC4.

On the other hand, the dimer/monomer ratio for FC4VFC4 increased with time from $t = 0$ min to 163 min to be greater than 0.5. After ER signal of FC4VFC4 showed a rapid decrease of the intensity, the dimer/monomer ratio value scattered. Note that the dimer/monomer ratios obtained from the ER spectra in 500 μM viologen aqueous solution on a bare Au electrode were 0.06 for C4VC4 and 0.22 for FC4VFC4. The enhanced dimerization in the Nafion film indicates the occurrence of concentration of these viologens in the ionic channels, and the extent of concentration became greater with time.

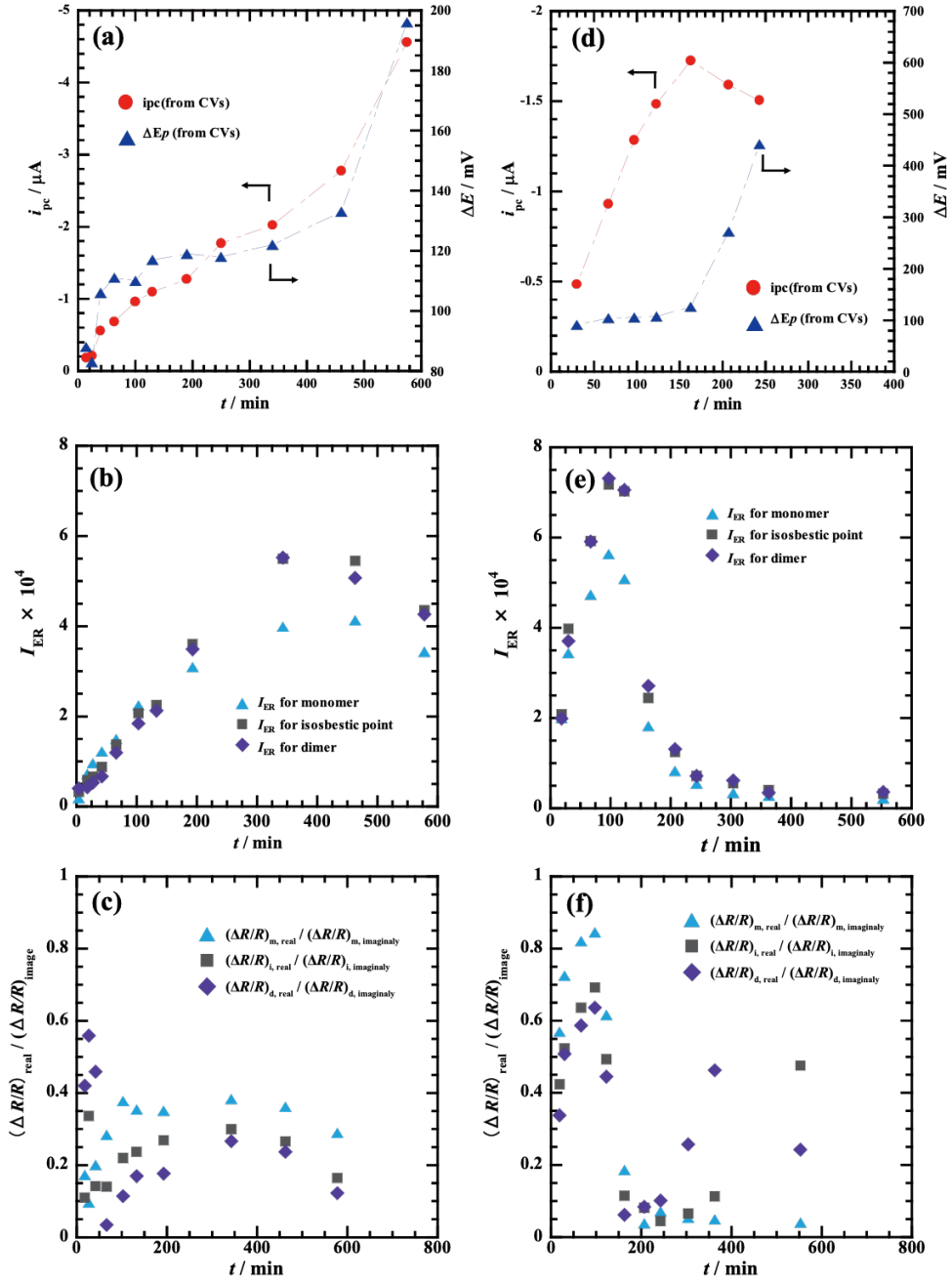

Fig. 5-7. Time dependence of the characteristic readout values from ER spectra and CVs in 50 μM C4VC4 + 0.1 M KCl solution (a, b, c) and 50 μM FC4VFC4 + 0.1 M KCl solution (d, e, f). (a) and (d): cathodic peak current i_{pc} and peak separation ΔE_p from CVs at 200 mV s^{-1}; (b) and (e), I_{ER} values (see Eq. 2) at three wavelengths, 603 nm as a monomer maximum in pale blue color triangles, 537 nm as a dimer maximum in gray squares, 552 nm as the isosbestic point in purple diamonds. (c) and (f) r/i ratios from ER spectra at the same three wavelengths as in (b) and (e).

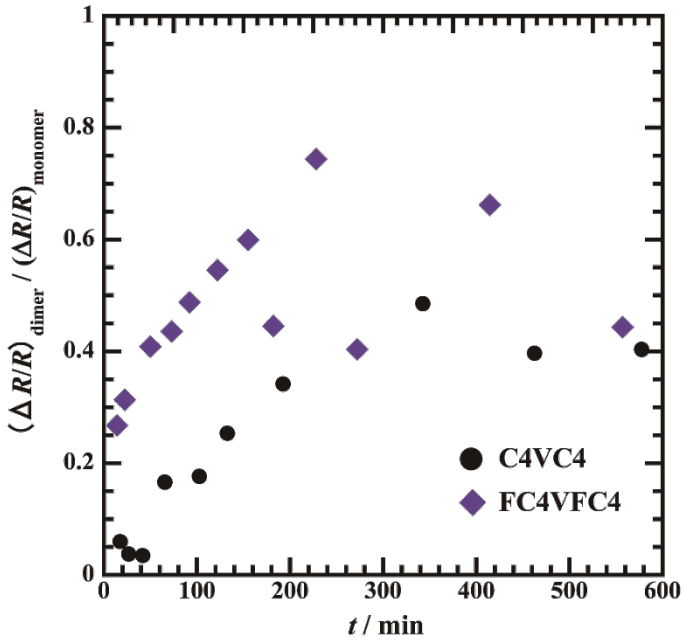

Fig. 5-8. Time-course dimer/monomer ratios calculated from ER spectra recorded in 50 μM C4VC4 + 0.1 M KCl solution (closed circle), in 50 μM FC4VFC4 + 0.1 M KCl solution (closed diamond).

5.3. Additional messages delivered by the redox probe FC4VFC4.

The results of several additional key experiments using FC4VFC4 were listed herein.

(i) We examined whether the potential scan affected the results of the time course experiments. A newly prepared Nafion-coated Au electrode was dipped in 500 μM FC4VFC4 solution, kept it at the open circuit for 1 h, and then subjected to an initial potential scan. We obtained irreversible response almost the same as the intermittent experiments (Fig. 5-2). Because viologen is not reduced at the open circuit potential, this fact indicates that the potential scanning condition is not the prerequisite of the time course phenomenon and that the increase in R_u takes place even when only V^{2+} permeated the Nafion film.

(ii) We examined the redox reaction of ruthenium hexamine complex in the Nafion film. We observed a reversible, diffusion-controlled response of $[Ru(NH_3)_6]^{2+/3+}$ at a Nafion-coated Au electrode in the solution of 500 μM $[Ru(NH_3)_6]Cl_3$ in the absence of viologen. Because

Nafion is a cation exchange membrane, abundantly incorporated $[Ru(NH_3)_6]^{2+/3+}$ underwent reversible redox reaction. When we changed the half of $[Ru(NH_3)_6]Cl_3$ to FC4VFC4 in the solution composition, the response of $[Ru(NH_3)_6]^{2+/3+}$ was largely diminished. The peak current of $[Ru(NH_3)_6]^{2+/3+}$ decreased to less than half, and ΔE_p became much greater, indicating a slower electron transfer rate of $[Ru(NH_3)_6]^{2+/3+}$. The final CV was of irreversible one. Note that no reduction of $[Ru(NH_3)_6]^{3+}$ mediated by viologen redox took place. When C4VC4 was used instead in the same experiment, apparent blocking of the redox of $[Ru(NH_3)_6]^{2+/3+}$ was not observed up to C_s of 500 μM.

(iii) We also examined CV response in the mixed viologen solutions, 250 μM MV + 250 μM FC4VFC4 and 250 μM C4VC4 + 250 μM FC4VFC4. In both solutions, the decay of the redox responses finally reached extremely irreversible ones as in Fig. 5-4-a. It is now clear that after the redox activity of FC4VFC4 is damped, even a coexistent smaller dialkylviologen cannot undergo quasi-reversible redox reaction.

(iv) We further examined the effect of relatively hydrophobic water-soluble cation and perfluoalkyl cations in the solution phase on the behavior of MV in a Nafion film. First, a Nafion film on a Au electrode was equilibrated in 500 mM MV solution to obtained steady-state CV. Then, in the electrolyte solution, added was 2 mM butyl trimethylammonium ($(CH_3)_3N^+$-C_4H_{10}) chloride or 2 mM *1H,1H,2H,2H*-perfluorobutyl trimethylammomium ($(CH_3)_3N^+$-C_2H_4-C_2F_5) chloride. The peak current eventually decreased to 88% of initial value for the former, whereas it decreased to 80% for the latter. Importantly, more hydrophobic, perfluorinated tetraaklylammomium cation penetrated the Nafion through the ionic channels and more effectively displaced pre-incorporated MV.

5. 4. Discussion on the experimental results and presumable models.

After the Nafion commenced to be used as a cation exchange and transport membrane of high performance following its invention in 1962, it has been long under debate how to understand the state and behavior of the cations in the ionic channels. The latest views can be found in literature. Wakai and co-workers discriminated three types of water in Nafion by using ^1H NMR, infrared, and mass spectroscopies, namely, condensed water, hydrated water,

and strongly bound water on the sulfonate group [16]. Interconversion among these three states may take place. Shia and co-workers discussed the interaction of the sulfonate group sites on the inner wall of the ionic channel with incorporated cations [17] in terms of the change of water content. They claimed that, large and multivalent cations such as Cs^+ and Mg^{2+}, being different from small monovalent cations such as Li^+, Na^+, and K^+, tend to localize at the sulfonate site. If the Nafion is not immersed in water but equilibrated in a low humidity atmosphere, the latter cations form cross-link structure together with sulfonate groups, because the localized interactive state behaves as an ion pair. But their discussion is limited to the case that electrostatic interaction is predominant.

Keeping these reports in mind, we describe a scenario of the time change of the state of viologens in the ionic channel in the Nafion film and the origin of the sharp contrast between perfluorinated viologen (FC4VFC4) and its alkyl analog (C4VC4). We have experimentally confirmed that both viologens can penetrate deep into the Nafion film to the electrode surface. It should be emphasized that the ionic channel of the Nafion can provide enough space for the $V^{\bullet+}$-forms to dimerize. In fact, the ER signal tracked both electroactive $V^{\bullet+}$-monomer and dimer species for both viologens (Figs. 5-8).

Because the total anionic charge of sulfonate groups in a Nafion film is constant, the increase of the incorporated amount of viologens leads to the decrease of K^+ concentration resulting in the increase of R_u. Regardless of the extent, this process takes place inevitably for both FC4VFC4 and C4VC4, and for MV as well. The viologen moiety is divalent (V^{2+}) or monovalent ($V^{\bullet+}$) cation being larger in size than the inorganic cations discussed in above mentioned work of Shia and coworkers [17]. Even when the Nafion film is hydrated in water, interaction between viologens and sulfonate groups should be significant.

The sharpest contrast between the two viologens is the fact that, although the redox response onsets and increases initially after immersion of the Nafion film in the solution, a turndown of redox activity of FC4VFC4 takes place. Not only the redox reaction of FC4VFC4 itself but also the reactions of smaller-in-size cationic species $[Ru(NH_3)_6]^{2+/3+}$ and MV were damped. This never happened for C4VC4 up to C_s = 500 μM. The redox activity is damped after CV curve becomes irreversible and ER signal disappears.

An important observation is given in (iv) of the section 3.4. Even the partly perfluorinated butyl trimethylammonium can penetrate in the ionic channel and displace pre-saturated MV in the Nafion film. This activity with partly perfluorinated butyl trimethylammonium was greater than the alkyl analog butyl trimethylammonium, indicating the contribution of the attractive interaction of the perfluorinated butyl with the perfluroalkyl-phase of Nafion following the penetration through the ionic channel. This process is in line with the penetration of FC4VFC4, resulting in the damping of the response of coexistent MV.

In addition, a threshold solution concentration of FC4VFC4 is in between 5 and 10 μM. At lower concentrations of FC4VFC4 than 10 μM, the CV does not become irreversible. The structural difference between the two viologens is whether the end ethyl groups are perfluorinated or not. Therefore, the significant difference in the redox behavior should originate from either or both intermolecular and FC4VFC4-Nafion perfluoro chain-chain interactions. The interactions do not work on C4VC4. Three possible models to describe the scenario can be proposed.

Model I. When the concentration of FC4VFC4 in the Nafion film is increased over a threshold, $V^{\bullet+}$ concentration as the reduction product reached its solubility limit in the ionic channels. We found in our previous work that FC4VFC4 has much lower aqueous solubility than C4VC4 because of intermolecular perfluoro chain-chain interaction [9]. This results in the precipitation in the film as C4VFC4-aggregates (Fig. 9) and a great extent of increase in R_u because of the narrowing of the ionic conductive pathways. Herein, predominant interaction is intermolecular perfluoro chain-chain interaction.

Model II. Both V^{2+}- and $V^{\bullet+}$-forms of $FC4V^{2+}FC4$ strongly stack to the inside-wall of the ionic channel through not only electrostatic cation-sulfate interaction but also perfluoro chain-chain interaction with Nafion perfluoroether side chains (Fig. 9). Recall that the hydration state in the ionic channel is physically supported by mutual electrostatic repulsion between sulfonate groups on the inner wall of the channel. The neutralization of the negative charges on the inner wall by extensive accumulation of viologens at the wall reduces electrostatic repulsion between sulfonate groups, resulting in the loss of the driving force to keep the ionic channel in a well-swollen, expanded state. Eventually, the ionic channels are narrowed, and R_u value becomes large.

Model III. Both intermolecular and FC4VFC4-Nafion perfluoro chain-chain interactions work synergistically. Aggregates of FC4VFC4 are produced because of the solubility limits. The aggregates undergo electrostatic and perfluoro chain-chain interaction with Nafion perfluoroether side chains (Fig. 9). Then, the ion channel is blocked.

Note that the Model I alone cannot explain the fact that, even when the electrode potential was kept at more positive potential of the formal potential of FC4VFC4, the CV became irreversible. To identify which model II or III is the most appropriate and to figure out which interaction is dominant or whether interactions are working synergistically or not, *in-situ* UV-visible and IR spectroelectrochemical measurements of the state of incorporated viologen are currently underway in our laboratory. The structure of ion channel in the presence of FC4VFC4 may be uncovered by using small angle X-ray Scattering and neutron reflection. Additionally, water uptake measurements *in an aqueous solution* should be needed.

In summary, FC4VFC4 gave us an unprecedented level of understanding of interaction of perfluoroalkyl cationic molecules with a Nafion film. Importantly, without the interactions brought about by the perfluoroalkyl chain, the electrostatic interaction alone does not induce apparent inhibition of the redox reaction.

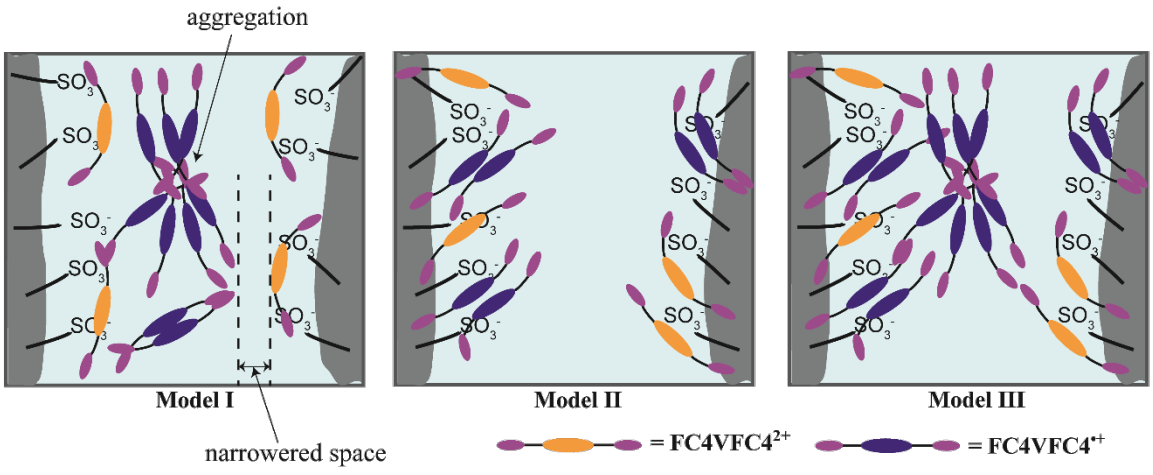

Fig. 5-9. Presumable models of the Nafion ion channel structure with saturated amount of FC4VFC4; **Model I**, FC4VFC4 aggregation model; **Model II,** Deposition on the inner wall surface model; **Model III,** Aggregation model including synergistically occurred deposition on the inner wall and FC4VFC4 aggregation.

5.5. Conclusions

Comparison of the redox behavior of FC4VFC4 and its alkyl analog C4VC4 was made in detail by a combined use of CV and ER. Because the difference between the two viologens was notable at the concentrations greater than 10 μM, our focus was on the range of higher concentrations. The results of the time course measurements after immersion of a freshly prepared Au/Nafion electrode into the viologen solutions of various concentrations gave us detailed information. Except for low concentrations (< 5 μM) of FC4VFC4, although the redox response onsets and initially increases, a turndown of redox activity of FC4VFC4 takes place. Not only the redox reaction of FC4VFC4 itself but also the reactions of $[Ru(NH_3)_6]^{2+/3+}$ and MV were damped. This never happened for C4VC4 up to C_s = 500 μM. The redox activity is damped after CV curve becomes irreversible and ER signal disappears. Without the interactions brought about by perfluoroalkyl chain, the electrostatic interaction alone does not induce apparent inhibition of the redox reaction. All the present experimental results and considerations allowed us to propose possible models in reference to recent reports. Those are Model II and III in Fig. 5-9, to describe the phenomena observed in this work. In conclusion, the new perfluorinated viologen probe provides us an unprecedented opportunity to shed deeper light into the interactions between organic cations and a Nafion film.

Refference (Chap. 5)

[1] M. Fujimura, T. Hashimoto, H. Kawai, Small-Angle X-ray Scattering Study of Perfluorinated Ionomer Membranes. 1. Origin of Two Scattering Maxima, Macromolecules 14 (5) (1981) 1309-1315.

[2] W.Y. Hsu, T. Gierke, Ion transport and clustering in Nafion perfluorinated membranes, J. Membr. Sci. 13 (3) (1983) 307-326.

[3] G. Gebel, Structural evolution of water swollen perfluorosulfonated ionomers from dry membrane to solution, Polymer 41 (15) (2000) 5829-5838.

[4] H.-G. Haubold, Th. Vad, H. Jungbluth, P. Hiller, Nano structure of NAFION: a SAXS study, Electrochim. Acta 46 (10-11) (2001) 1559-1563.

[5] L. Rubatat , A.L. Rollet , G. Gebel , O. Diat, Evidence of Elongated Polymeric Aggregates in Nafion, Macromolecules 35 (10) (2002) 4050-4055.

[6] K.S. Rohr, Q. Chen, Parallel cylindrical water nanochannels in Nafion fuel-cell membranes, Nat. Mater. 7 (2008) 85-83.

[7] K. D. Kreuer, G. Portale, A Critical Revision of the Nano-Morphology of Proton Conducting Ionomers and Polyelectrolytes for Fuel Cell Applications, Adv. Funct. Mater. 23 (43) (2013) 5390-5397.

[8] M. Inaba, J.T. Hinatsu, Z. Ogumi, Z. Takehara, Application of the Solid Polymer Electrolyte Method to Organic Electrochemistry: XV. Influence of the Multiphase Structure of Nafion on Electroreduction of Substituted Aromatic Nitro Compounds on Cu,Pt Nafion, J. Electrochem. Soc. 140 (3) (1993) 706-711.

[9] T. Ayabe, B. Chan, T. Sagara, Fluorination effect of dibutyl viologen on its electrochemistry in aqueous solution, J. Electroanal. Chem. 856 (2020) 113691 1-6.

[10] P. N. Pintauro, R. Tandon, L. Chao, W. Xu, R. Evilia, Equilibrium Partitioning of Monovalent/Divalent Cation-Salt Mixtures in Nafion Cation-Exchange Membranes, J. Phys. Chem 99 (34) (1995) 12915-12924.

[11] X. Tang, T.W. Schneider, J.W. Walker, D.A. Buttry, Dimerized π-Complexes in Self-Assembled Monolayers Containing Viologens: An Origin of Unusual Wave Shapes in the Voltammetry of Monolayers, Langmuir 12 (24) (1996) 5921-5933.

[12] P. Bertoncello, P. Ugo, Preparation and Voltammetric Characterization of Electrodes Coated with Langmuir-Schaefer Ultrathin Films of Nafion, J. Braz. Chem. Soc. 4 (14) (2003) 517-522.

[13] T. Sagara: In Advances in Electrochemical Science and Engineering, Vol. 9, Eds. C. Alkire, D. M. Kolb, J. Lipkowski, P. N. Ross, Wiley-VCH Verlag, Weinheim, pp. 47-95 (2006).

[14] T. Sagara, H. Murase, N. Nakashima, Frequency dependence of the electroreflectance signal for redox reaction of solution-phase species at the electrode surface: Formulation and experimental verification, J. Electroanal. Chem. 454 (1/2) (1998) 75-82.

[15] C. Gao, S. Silvi, X. Ma, H. Tian, A. Credi, M. Venturi, Chiral Supramolecular Switches Based on (*R*)-Binaphthalene–Bipyridinium Guests and Cucurbituril Hosts, Chem. Eur. J. 18(2012) 16911-16921

[16] C. Wakai, T. Shimoaka, T. Hasegawa, ^{1}H NMR Analysis of Water Freezing in Nanospace Involved in a Nafion Membrane, J. Phys. Chem. B 119 (25) (2015) 8048-8053.

[17] S. Shia, A. Z. Webera, A. Kusoglu, Stracture-transport relationship of perfluorosulfonic-acid membranes in different cationic forms, Electrochim. Acta 220 (1) (2016) 517-528.

Chapter 6

Effect of Underlying Monolayers on Redox Reaction of Methyl Viologen at Nafion Film modified Au Electrode

ABSTRACT. Three different self-assembled monolayers of alkylthiol derivatives (SAMs) were formed on a polycrystalline Au electrode before casting a Nafion thin film. Immersing the modified electrode in methyl viologen (MV) aqueous solution, redox reactions of MV at the Au/SAM/Nafion interfaces were characterized using the results of the voltammetric and electroreflectance measurements. The voltammetric currents at a Au/perfluoro-terminated alkyl SAM/MV solution interface was ca. 90% of that at a Au/MV solution interface. In sharp contrast, the current at a Au/perfluoro-terminated alkyl SAM/Nafion/MV solution interface was approximately the half of that at the Au/Nafion/MV solution interface, showing a stronger blocking effect when the SAM is in contact with Nafion. The implications of the variety of the effects of the SAMs underlying the Nafion film were discussed. The results in this work showed the importance of the approach to insert a SAM in between conductive materials such as metallic catalysts and Nafion films.

6.1. Introduction

Nafion® is the most widely used functional cation exchange polymer for various applications such as proton transporting membranes, sensors, and supporting materials for catalysts. Nafion coatings on catalysts have been an important approach to enhance the activity and selectivity [1, 2]. When one needs to regulate the electron or proton transfer at a catalyst/Nafion interface, insertion of a self-assembled monolayer (SAM) in between would be an important method of choice. It would be as a promising mean to optimize the electron and proton transfer processes as well as film micro-structures. Cha et al. used an alkanethiol SAM on a Au electrode to reinforce the adhesion of the Nafion film without degradation of the redox of cationic species across the film [3]. After their work, however, the merits and problems in the use of the electrode/SAM/Nafion structure and its electrochemical characteristics have been left unanswered.

A solid/Nafion interfacial structure depends on the chemical nature of the substrate and atmosphere for the processing. The examples include humidity dependent formation of an interlaminated structure of water-rich layers and fluoroalkyl phase layers on a SiO_2 hydrophilic surface [4], substrate surface chemistry dependent abundance and connectivity of water-filled proton conducting channels in Nafion films [5], and the effect of an *n*-octyltrichlorosilane layer on the orientation of the ion-channels [6]. Most likely, a thin SAM underlayer also affects the properties and electrochemistry of a thick Nafion overlayer.

In this chapter, we explore the effect of the pre-modification of the electrode surface by SAMs before casting a Nafion film (ca. 1 μm-thick) upon the electrochemistry of cationic species.

6.2. Results and Discussion

Before casting Nafion on a polished polycrystalline Au electrode surface (0.0201 cm^2), formed was one of the three SAMs of alkyl thiol derivatives: 1-decanethiol (C10-SH), ω-hydroxy-hexanethiol (HO-C6-SH), and *1H,1H,2H,2H*-perfluoro-1-decanethiol

(Perfluoro-C10-SH). The last one is used to see the perfluoro-interaction between the SAM and the perfluoro-phase region in the Nafion film in reference to our previous reports [7, 8]. The Au electrode was modified by a SAM in 1 mM ethanoic solution of one of the three thiol compounds for 12 h. The Au/SAM/Nafion interfaces were characterized in the solution of methyl viologen (MV) as a redox probe by combined use of voltammetric and ER measurements [9]. A Nafion 5 wt.% solution and the three alkyl thiol derivatives were purchased from Sigma Aldrich. MV dichloride salt was home synthesized.

When casting Nafion dispersion, the Au/SAM was inevitably brought into contact with 2-propanol, because it is the solvent of the Nafion dispersion. To see whether the immersion in 2-propanol deteriorates the SAM, cyclic voltammograms (CVs) of the Au/SAM electrodes in 0.050 mM MV aqueous solution were measured before and after immersing the electrodes in 2-propanol for 2 hr. A three-electrode configuration with a Ag|AgCl|sat'd KCl reference electrode and a coiled Au wire counter electrode was used under an Ar gas (> 99.998%) atmosphere at 25 ± 2°C. The base supporting electrolyte was 0.10 M KCl (M = mol dm^{-3}) prepared from reagent grade KCl (Nacalai) and milli-Q water.

Immersion of a Au/HO-C6-SH electrode in 2-propanol turned out an approximately doubled CV peak current of the MV redox, a decrease in the separation between anodic and cathodic CV peak potentials (ΔE_p) from 69 to 63 mV at v =200 mV/s, and a tripled double-layer capacitance of 17 μF cm^{-2} at 0.1 V. The other two Au/SAM showed no apparent change in the same immersion test. We excluded the use of HO-C6-SH thereafter because of the instability of its SAM.

On a bare Au electrode and SAM-covered electrodes without pre-immersion in 2-propanol, Nafion film coating was made by casting 0.5 wt% Nafion/2-propanol solution and drying in air for 2 hr to attain 1.0 ± 0.2 μm dry-state thickness as measured by AFM. The film showed a continuous and homogeneous light-interference pattern. Before use, the Nafion film on the electrode was swelled by immersing it in MV-free KCl solution. The time zero (t = 0 min)

was set when a Nafion-coated electrode was immersed in a pre-deaerated MV solution. At certain times, a single potential-cycle CV was recorded at v = 200 mV s^{-1}. The details of the combined CV and ER train measurements were fully described in our previous reports [8].

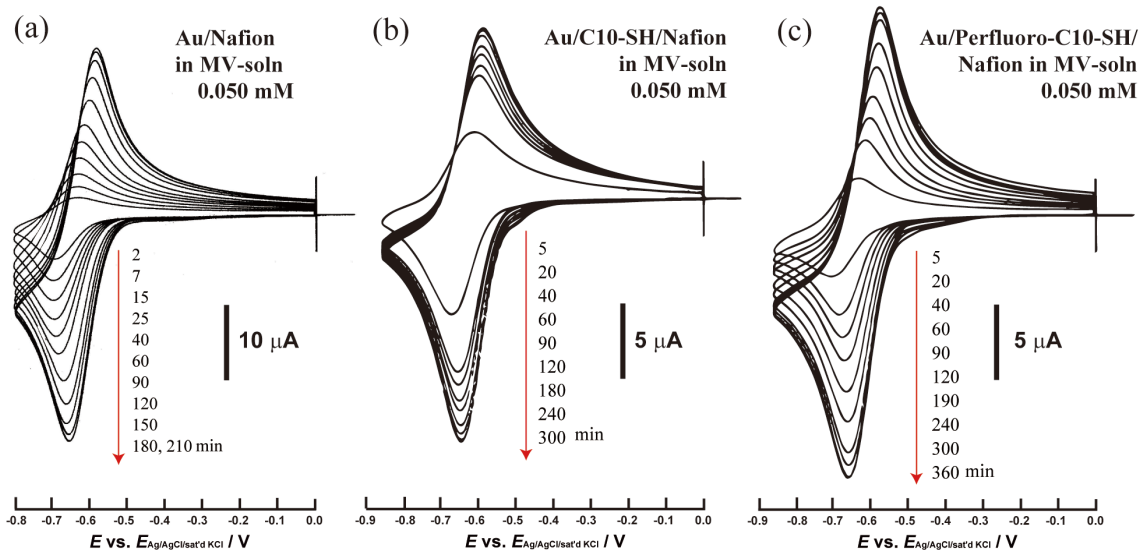

Figure 6-1. Time course CVs at Au/Nafion (a) and Au/SAM/Nafion systems (b and c) at v = 200 mV s^{-1}.

Table 6-1. Characteristic of CV response in 0.05 mM MV solution at v = 200 mV s^{-1}.

Before Nafion coating *			With Nafion coating **		
Electrode	$-i_{pc}$ / μA	ΔE_p / mV	underlayer SAM	$-i_{pc}$ / μA	ΔE_p / mV
bare Au	0.30	66	none	29	72
Au/C10-SH	0.29	65	C10-SH	15.5	57
Au/Perfluoro-C10-SH	0.22	86	Perfluoro-C10-SH	16.3	85

*After 2 hr-immersion in 2-propanol

**Data after saturation obtained in the same experiments in Figure 2 (vide supra).

The time course CVs are shown in Fig. 6-1. In the first scan CV at Au/Nafion at t = 2 min, a redox peak pair appeared with the midpoint potential, E_m, of -0.670 V of viologen radical cation/dication ($V^{\bullet+}/V^{2+}$) redox couple. Because a bare Au electrode gives E_m = -0.623 V, the CV revealed no appreciable existence of pores to give direct contact of the MV solution to the bare part of the Au surface.

Table 6-1 shows the characteristics of CV before Nafion coating and after saturation with Nafion coating. All the voltammetric peak currents (represented by cathodic peak current, i_c, in Table 1) were proportional to $v^{1/2}$, indicating that the redox reactions are largely controlled by diffusion. Before Nafion coating, the Perfluoro-C10-SH SAM showed a weak blocking against redox of MV, while C10-SH did not. Approximately 100 times as much reversible current response at Au/Nafion as at bare Au indicates that the product of MV concentration and the square root of the apparent diffusion coefficient, D_{app}, of MV in the Nafion film is 100 times greater than in solution, provided that the whole electrode surface area is active. Because D_{app} is four order of magnitude smaller in the film than in the solution [10], over two order of magnitude of MV concentration occurred in the present condition.

Time course changes of - $i_{pc,}$ ΔE_p, E_m, and the content of MV dimer (f_{dimer}) are shown in Fig. 6-2. As shown in Figs. 6-1 and 6-2, the CVs of three systems reached saturation in 150-250 min after immersion. From ER spectra, we can calculate f_{dimer} as the number of viologen units in dimer of $V^{\bullet+}$ relative to all the electroactive viologen units using the signals at 603 and 537 nm [11].

The pieces of important information in regard to the comparison of the three systems we obtained from these results include:

(1) Almost the same f_{dimer} reveals nearly the same concentration of MV in the ionic channels.

(2) The micro-environments for MV are also nearly the same because of the coincidence of the E_m values.

(3) On the basis of ΔE_p, because diffusion coefficient of MV in the bulk of Nafion cannot be lowered by the insertion of the SAM, the interfacial electron transfer rate constant is greater for C10-SH but smaller for Perfluoro-C10-SH than that at Au/Nafion.

(4) Therefore, additionally taken the same level of saturated i_{pc} for the two SAMs, being about half of i_c at the Au/Nafion system, C10-SH accelerates the interfacial electron transfer but reduces the number of ionic channels on its SAM surface. On the other hand, whereas Perfluoro-C10-SH slowed the interfacial electron transfer process but did not decrease or even increased the number of ionic channels in the Nafion film on its SAM surface. This may originate from the perfluoro affinity between the Perfluoro-C10-SH SAM terminal group and the perfluoro phase of Nafion, whereas the details should be clarified in due course. The

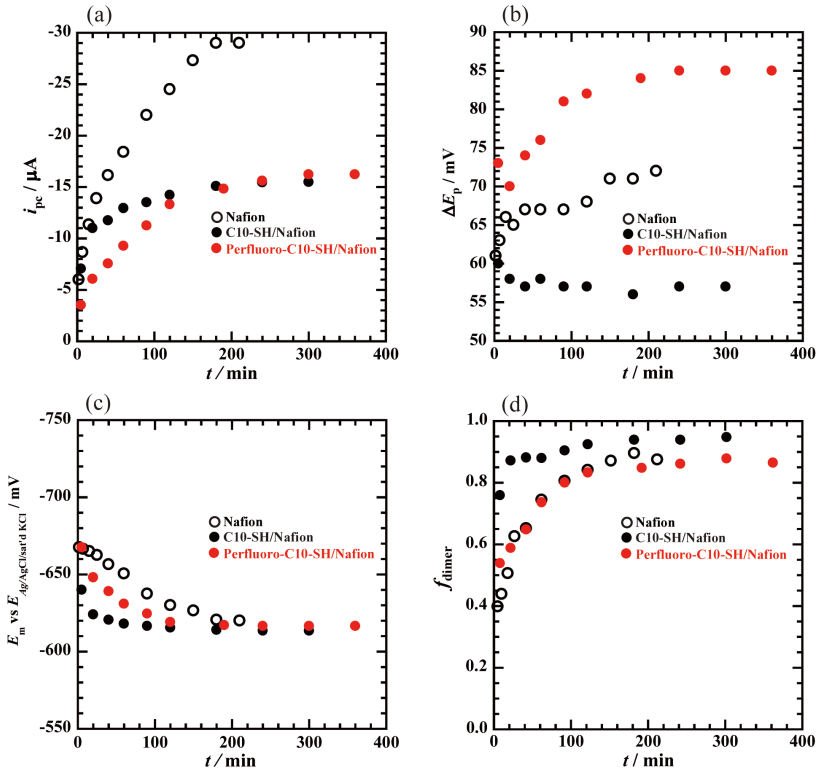

Figure 6-2. Characteristics of voltammetric response (a-c) obtained from the CVs and the fraction of viologen unit in dimer form (d) obtained from ER spectra for the three systems notified in the figure in 0.050 mM MV + 0.1 M KCl.

surface chemistry-dependent growing of the covering area by the water-rich ion-channel on the electrode was reported by Ohira and colleagues [4]. Our above-mentioned result is in line with the claim of Ohira and colleagues. The use of Perfluoro-C10-SH SAM for the reinforcement of the double layer structure does not negatively affect electron transfer processes in/through Nafion.

6.3. Conclusions

In summary, we have evaluated the effect of insertion of the SAMs in between the Au electrode surface and Nafion film on the redox processes of MV in the film using voltammograms and ER spectra. The time course of the redox response was monitored until saturation. We gained insights into the insertion effect on the density of active ionic channels and the heterogeneous electron transfer kinetics. We further need to shed light on the molecular level structure of SAM/Nafion interfaces in due course, because we found clearly the terminal group dependence in this preliminary study.

6.4. Supporting Information

6.4.1 Electroreflectance (ER) spectra

Typical ER spectra for a Au/Nafion and two Au/SAM/Nafion systems are shown in Figure S1. These spectra always showed a difference absorption spectral feature. The ER spectrum was in accord with the absorption spectrum at more negative potential, from which the spectrum at less negative potential was subtracted[1]. A much greater imaginary part than the real counterpart indicated that ER monitored the viologen redox both at the proximity to the surface and in the diffusion layer in the Nafion film [1,2]. Taking a look at the spectral structure, although absorption of $V^{\bullet+}$-monomer (wavelength of absorption maximum: λ_{max} = 603 mm) was recorded as well as that of $V^{\bullet+}$-dimer (λ_{max} = 537 mm) in the first 10 min after immersion in 0.05 mM MV solution, absorption of $V^{\bullet+}$-dimer became dominant after that. From each ER spectrum, we can calculate the fraction of the viologen units in dimer of $V^{\bullet+}$ relative to all the electroactive viologen units, f_{dimer}, using the signals at 603 and 537 nm [3].

Note that the isosbestic point of the monomer and dimer absorptions is at 552 nm, representing total amount of viologen units being active under the potential modulation. Progressive domination of $V^{\bullet+}$-dimer over $V^{\bullet+}$-monomer was observed in all three systems.

6.4.2 Atomic force microscope (AFM) measurement for estimating Film thickness

For estimating Nafion film thickness, AFM measurement was conducted for Nafion film modified on Au substrate using scratching method. AFM image for Au/Nafion shown at Figure S6-2 (a), and the depth profile of white line in Figure S6-2 (a) shown at Figure S6-2 (b). The valley on right edge of Figure S6-2 (a) is the scratch by cutter, it can be found that the depth of the scratch is about 1 μm from the depth profile (Figure S6-2 (b)).

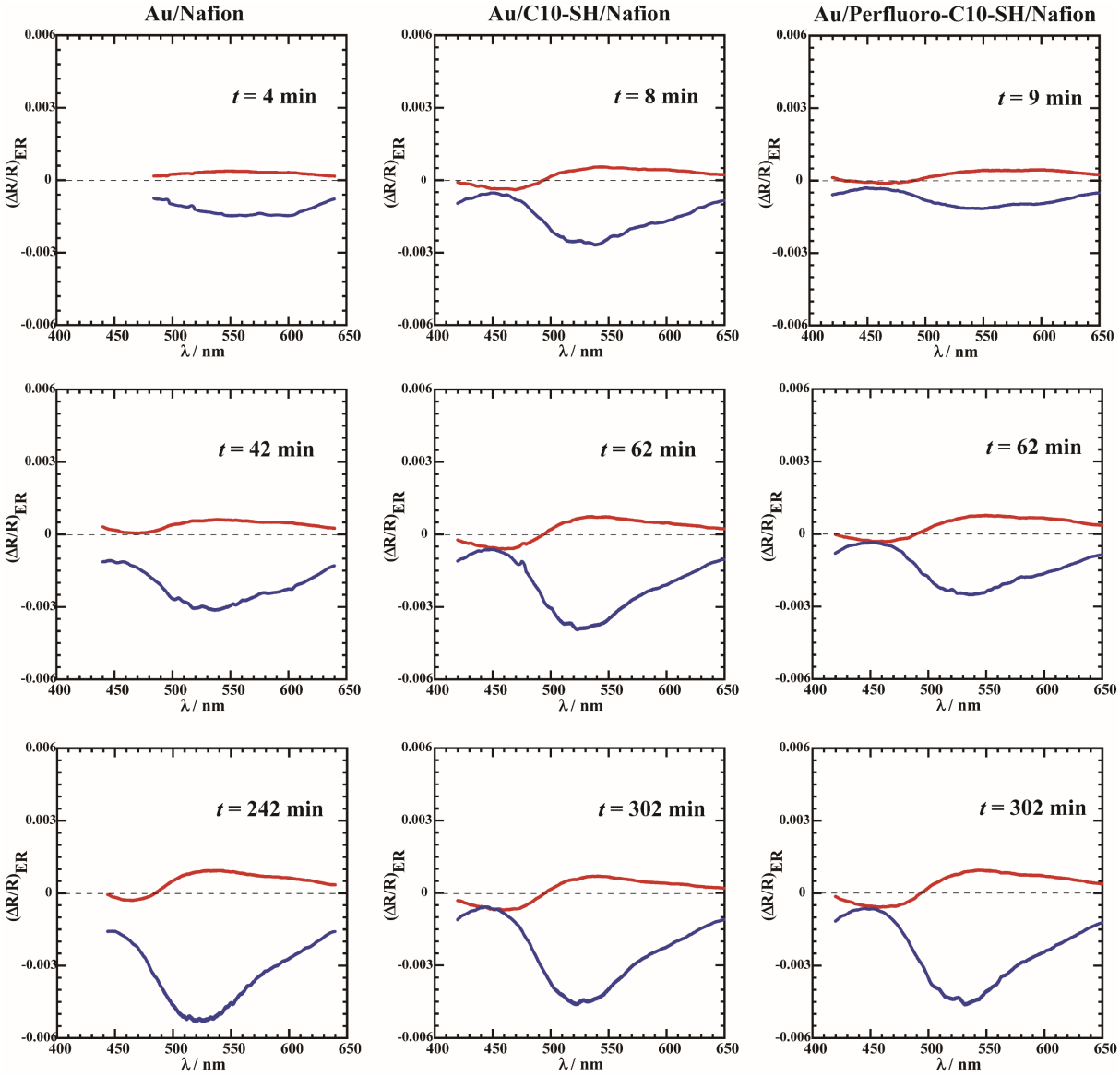

Figure S6-1. ER spectra for a Au/Nafion and two Au/SAM/Nafion systems in 0.050 mM MV + 0.1 M KCl solution. The dc potential was set to be the same as the midpoint potential of the latest cyclic voltammogram, the potential modulation frequency was 14.0 Hz, the zero-peak amplitude was 56 mV, and the wavelength (λ) scan rate was -2 nm/s. The time points of the measurements after immersion of the electrode are noted in each spectrum.

(a)

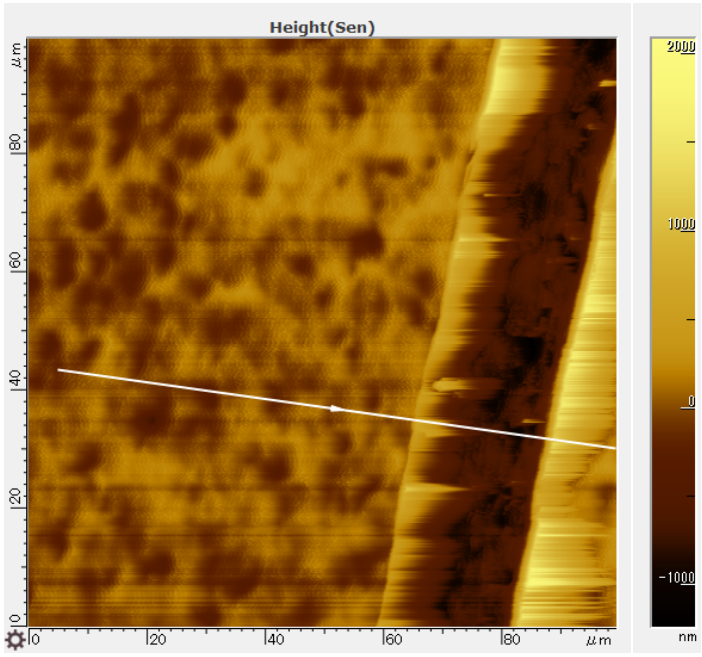

(b)

Figure S6-2. AFM image for a Nafion film modified on Au substrate (a), and the depth profile at white line (b).

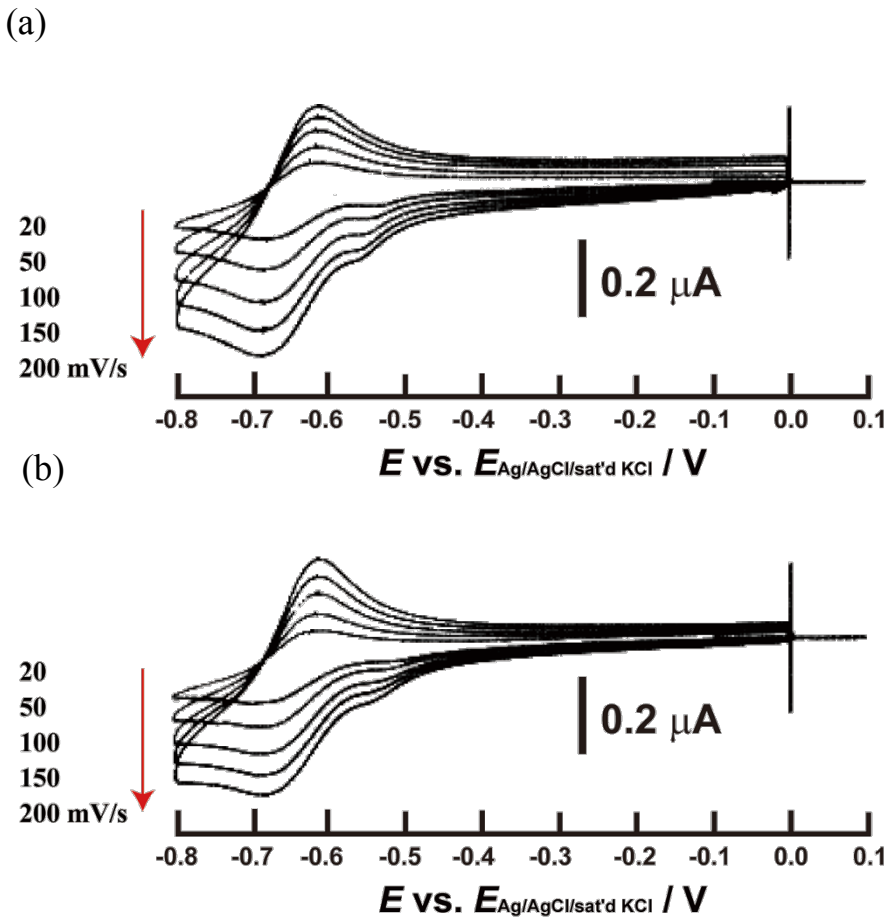

Figure S6-3. CVs at Au/SAM systems in 0.05 mM MV + 0.1 M KCl solution, (a) Au/C10-SH and and (b) Au/FC10-SH. For both (a) and (b), v = 200, 150, 100, 50, 20 mV s-1.

Refference (Chap. 6)

[1] A. Chen and P. Holt-Hindle, Platinum-Based Nanostructured Materials: Synthesis, Properties, and Applications, Chem. Rev. 110 (2010) 3767-3804.

[2] J.-F. Huang and W.-R. Chang, Cu(i)-mediating Pt reduction to form Pt-nanoparticle-embedded Nafion composites and their electrocatalytic O_2 reduction, J. Mater. Chem. 22, (2012) 17961-17966.

[3] C. S. Cha, J. Chen, and P. F. Liu, Improvement of the adhesion of a Nafion® modifying layer on electrodes, J. Electroanal. Chem. 345 (1993) 463-467.

[4] J. A. Dura, V. S. Murthi, M. Hartman, S. K. Satija, and C. F. Majkrzak, Multilamellar Interface Structures in Nafion, Macromolecules 42 (2009) 4769-4774.

[5] A. Ohira, S. Kuroda, H. F. M. Mohamed, and B. Tavernierb, Effect of interface on surface morphology and proton conduction of polymer electrolyte thin films, Phys. Chem. Chem. Phys. 15 (2013) 11494-15000.

[6] M. A. Modestino, A. Kusoglu, A. Hexemer, A. Z. Weber, and R. A. Segalman, Controlling Nafion Structure and Properties via Wetting Interactions, Macromolecules 45 (2012) 4681-4688.

[7] T. Ayabe, B. Chan, and T. Sagara, Fluorination effect on electrochemistry of dibutyl viologen in aqueous solution, J. Electroanal. Chem. 856 (2020) 113691.

[8] T. Ayabe, A. Chen, and T. Sagara, Electrochemical and spectroelectrochemical probing of the ionic channel in Nafion films using the redox of perfluoroalkyl viologen, J. Electroanal. Chem. 873 (2020) 114442.

[9] T. Sagara, Diffraction and Spectroscopic Methods in Electrochemistry (Eds. C. Alkire, D. M. Kolb, J. Lipkowski, and P. N. Ross), Advances in Electrochemical Science and Engineering, 9, Wiley-VCH Verlag, Weinheim, pp. 47–95 (2006).

[10] A. M. Hodges, O. Johansen, J. W. Mer, A. W.-H. Mau, J. Rabani, and W. H. F. Sasse, Diffusion of viologens in Nafion film studied by a combined electrochemical-spectrophotometric method, J. Phys. Chem. 95 (1991) 5966-5970.

[11] B. C. Patterson and J. K. Hurst, Pathways of viologen-mediated oxidation-reduction reactions across dihexadecyl phosphate bilayer membranes, J. Phys. Chem. 97 (1993) 454-465

Refference in Supporting Information (Chap. 6)

[1] T. Sagara, in: Diffraction and Spectroscopic Methods in Electrochemistry (Eds. C. Alkire, D.M. Kolb, J. Lipkowski, and P.N. Ross), Advances in Electrochemical Science and Engineering, 9, Wiley-VCH Verlag, Weinheim, pp. 47–95 (2006).

[2] T. Sagara, H. Murase, and N. Nakashima, Frequency dependence of the electroreflectance signal for redox reaction of solution-phase species at the electrode surface: formulation and experimental verification, J. Electroanal. Chem. 454 (1998) 75-82.

[3] B. C. Patterson and J. K. Hurst, Pathways of viologen-mediated oxidation-reduction reactions across dihexadecyl phosphate bilayer membranes, J. Phys. Chem. 95 (1993) 454-465.

Chapter 7

Conclusion

7. Summary and Future Prospects

In this thesis, a viologen that has fluorinated sidechains is newly synthesized and used for the molecule probe for unveiling micro chemical environments of Nafion. Additionally, the effect of insertion of the SAMs in between the Au electrode surface and Nafion is investigated from the electrochemical response and ER spectra of introduced methyl viologen.

A detailed investigation of the electrochemistry of the perfluorinated viologen (FC4VFC4) in aqueous solution, and its results have been described. The investigation which reveals the effect of sidechain fluorination on the physicochemical properties. The oxidized form of FC4VFC4 has a more positive formal potential and a lower diffusion coefficient in water than C4VC4. The positive shift of formal potential $E^{o'}$ arose from strong electron-withdrawing effect of the perfluorinated groups, despite a separation of $(CH_2)_2$ from the viologen core. Two probable contributing factors to the positive shift are considered: (1) contribution of C_2F_5 unit to the electron-accepting LUMO, and (2) long-range electrostatic/inductive effects of the C_2F_5 unit. Our DFT computations indicate that the latter effect is substantial, with a C_2F_5 unit showing considerable effects on $E^{o'}$ for substrates with up to approximately ten CH_2 units of separation. The lower D_{ox} of FC4VFC4 when compared with C4VC4 is not likely to be a result of conformational differences of the two molecules in water. We find that the fluorinated compounds to be generally less soluble in water than their hydrocarbon counterparts. Our calculations suggest that fluorination facilitate solvation of bare ion pair of the viologen and its counter ions. The stronger binding with the counter ions, however, gives rise to a lower solubility than the non-fluorinated viologen species.

FC4VFC4 was incorporated in a Nafion film to explore the chemical micro-environment. Fluorination of dibutyl viologen induced distinct increasing irreversibility of redox reaction in Nafion. The irreversible redox reaction of FC4VFC4 was shown at relatively high concentrations (500 μM, 50 μM, 20 μM, 10 μM), but at low concentration (5 μM), quasi-reversible response was shown. In the ER-CV time-course measurements, I_{ER} at 50 μM

FC4VFC4 + 0.1 M KCl solution finally disappeared as opposite to steady-state time-course behavior of C4VC4. The dimer/monomer ratio calculated from time-course results indicate increasing concentration in the case of FC4VFC4 and C4VC4. Overall, we consider that the irreversible response of CV and ER signal disappearance in FC4VFC4 aqueous solution indicates R_u increasing by presumable models.

Additionally, we have evaluated the effect of insertion of the SAMs in between the Au electrode surface and Nafion film on the redox processes of MV in the film using voltammograms and ER spectra. The time course of the redox response was monitored until saturation. We gained insights into the insertion effect on the density of active ionic channels and the heterogeneous electron transfer kinetics. We further need to shed light on the molecular level structure of SAM/Nafion interfaces in due course, because we found clearly the terminal group dependence in this preliminary study.

Although some points remaining unexploited, the results obtained in this doctoral dissertation research unveiled new nature of Nafion and is useful for controlling interface structure between Nafion and electrode. Especially, the results that ion conductivity of Nafion film has apparent threshold to FC4VFC4 concentration in Nafion indicate the possibility of providing switching function of proton conduction to Nafion film. Further attempting to choose introduced molecule in Nafion will make ON/OFF switching proton conductivity by redox reaction of the introduced molecule possible. The redox induced ON/OFF switching proton conductivity of Nafion can be the analogous element for ion channel gate of cell membrane, it is expected to play a role in new energy conversion system that mimic biological system.

List of Publications

[1] Tatsuya Ayabe, Bun Chan, Takamasa Sagara, “Fluorination effect on electrochemistry of dibutyl viologen in aqueous solution”, *Journal of Electroanalytical Chemistry*, **856**, 1-6 (2020).

[2] Tatsuya Ayabe, Aicheng Chen, Takamasa Sagara, “Electrochemical and spectroelectrochemical probing of the ionic channel in Nafion films using the redox of perfluoroalkyl viologen”, *Journal of Electroanalytical Chemistry*, **873**, 1-12 (2020).

[3] Tatsuya Ayabe, Takamasa Sagara, “Effect of Underlying Monolayers on Redox Reaction of Methyl Viologen at Nafion Film Modified Au Electrode”, *Electrochemistry,* **89**, 131-133 (2021).